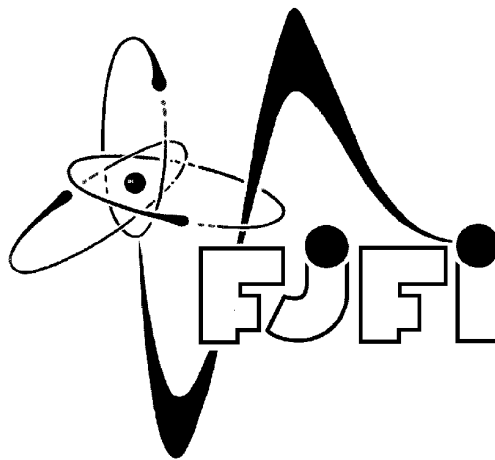


CZECH TECHNICAL UNIVERSITY IN PRAGUE

FACULTY OF NUCLEAR SCIENCES AND
PHYSICAL ENGINEERING

DEPARTMENT OF PHYSICS



DIPLOMA THESIS

Antikaon–Nucleus Interaction

Daniel Gazda

Prague 2007

Acknowledgments

I would like to express my gratitude to my supervisor Jiří Mareš for his guidance and hours of discussions upon conception of this diploma thesis and for sharing with me his insight into physics.

This work was supported by the GA AVCR grant IAA100480617.

My last and personal words of thanks belong to my parents and Aneta for their endless patience, love and encouragement, which enabled me to complete this thesis.

Declaration of originality

I declare that I have written this diploma thesis independently using the listed references.

I agree with using this diploma thesis.

Prohlašuji, že jsem svou diplomovou práci vypracoval samostatně a použil jsem pouze podklady (literaturu, projekty, SW atd.) uvedené v příloženém seznamu.

Nemám závažný důvod proti užití tohoto školního díla ve smyslu § 60 Zákona č.121/2000 Sb., o právu autorském, o právech souvisejících s právem autorským a o změně některých zákonů (autorský zákon).

V Praze dne

.....
podpis

Title: Antikaon–nucleus interaction

Author: Daniel Gazda

Specialization: Nuclear engineering

Supervisor: RNDr. Jiří Mareš CSc., Nuclear Physics Institute ASCR

Abstract: The subject of the present work is the study of the K^- meson interaction with the nuclear medium. The K^- –nuclear states were generated across the periodic table and calculated selfconsistently within the framework of the relativistic mean-field theory. A wide range of the K^- binding energies was spanned by varying the K^- couplings to the meson fields. The K^- absorption in the nuclear medium was taken into account using the optical model phenomenology. The strength of the absorptive potential was constrained by kaonic atom data and the phase space reduction for decay products of the K^- bound states was considered. We aimed at a detailed analysis of processes and conditions, which determine the K^- decay width. Significant contribution from the $\bar{K}N \rightarrow \pi\Lambda$ conversion mode was found for the \bar{K} binding energies in the range, where the dominant decay channel $\bar{K}N \rightarrow \pi\Sigma$ is closed. The assumption of the ρ^2 density dependence for the $2N$ -absorption modes leads to further increase of the K^- conversion width, especially for deeply bound K^- –nuclear states in lighter nuclei. Calculations of nuclear systems containing several antikaons revealed that antikaon and nuclear densities behave quite regularly with increasing number of K^- mesons, embedded in the nuclear medium. The study of the p -wave interaction of the K^- meson with a nucleus indicates that the p -waves play a minor role in heavier nuclear systems.

Keywords: K^- –nuclear bound states, density dependent interaction, relativistic mean-field model

Název práce: Interakce antikaonu s jádrem

Autor: Daniel Gazda

Studijní obor: Jaderné inženýství

Vedoucí práce: RNDr. Jiří Mareš CSc., Ústav jaderné fyziky AVČR, v. v. i.

Abstrakt: Předmětem předkládané práce je studium interakce K^- mesonů s jaderným prostředím. Jaderné stavy K^- mesonů byly studovány napříč periodickou tabulkou v rámci relativistické teorie středních polí. Pokryli jsme široké spektrum vazbových energií K^- mesonů škálováním vazbových konstant antikaonu na mesonová pole. Absorpce K^- mesonu byla zahrnuta prostřednictvím fenomenologického optického modelu. Hloubka imaginárního potenciálu byla určena z dat kaonových atomů, navíc jsme vzali do úvahy redukci fázového prostoru pro rozpadové produkty vázaných stavů. Zaměřili jsme se na detailní analýzu procesů a podmínek, které určují rozpadovou šířku K^- mesonu. Nalezli jsme významný příspěvek do rozpadové šířky K^- mesonu, pocházející z konverze $\bar{K}N \rightarrow \pi\Lambda$ pro oblast vazbových energií K^- , kde je hlavní rozpadový kanál $\bar{K}N \rightarrow \pi\Sigma$ kinematicky uzavřen. Ukázali jsme, že předpoklad kvadratické hustotní závislosti dvou-nukleonového absorpčního kanálu vede k dalšímu růstu rozpadové šířky K^- mesonu, obzvláště pro hluboko vázané stavy K^- v lehčích jádrech. Výpočty jaderných systémů obsahující více K^- mesonů ukázaly regulární chování jaderné hustoty s rostoucím počtem vázaných K^- mesonů. Studium vlivu započtení p -vlny do interakce K^- mesonu s jádrem prokázalo malý vliv p -vlny v těžších systémech.

Klíčová slova: vázné jaderné stavy K^- , hustotně závislá interakce, relativistická teorie středních polí

Contents

1	Introduction	1
2	Methodology	5
2.1	RMF model	5
2.2	Optical model phenomenology	11
3	Results and discussion	14
3.1	Effects of additional meson fields	14
3.2	Optical model modifications	17
3.3	Systems with more antikaons	21
4	Summary	26
	References	28
	Appendices	31
A	Notation and conventions	31
B	Conserved currents	32
C	Numerical solution	35

1 Introduction

The subject of the present work is the study of the K^- meson interaction with the nuclear medium. It is closely related to the one of the most important, yet unsolved, problems in hadron physics – how the hadron masses and interactions change within the nuclear medium.

The in-medium properties of antikaons in dense nuclear matter have attracted considerable attention since the pioneering work of Kaplan and Nelson on the possibility of kaon condensation in nuclear matter [1, 2].

The existence of the $\bar{K}N$ $\Lambda(1405)$ quasi-bound state lying about 27 MeV below the K^-p threshold suggests that the $\bar{K}N$ interaction is strongly attractive [3]. This is consistent with low-energy $\bar{K}N$ scattering data [4] as well as with the measured energy shifts of the $1s$ atomic state of kaonic hydrogen [5]. The $\Lambda(1405)$ as a K^-p quasi-bound state was also corroborated in a meson exchange picture by Jülich group [6], where the σ and ω mesons act jointly to give strong attraction. The chiral $SU(3)$ calculations showed that $I = 0$ $\bar{K}N$ interaction is attractive enough to bound $\Lambda(1405)$ [7].

The \bar{K} -nucleus interaction is also strongly attractive (and absorptive), as derived from the strong-interaction shifts and widths in kaonic-atom levels [8, 9, 10, 11, 12]. This claim is further supported by enhanced production of K^- mesons observed in sub-threshold and near-threshold heavy-ion collisions in the KaoS experiment at GSI [13, 14, 15]. Global fits of the kaonic-atom data based on a phenomenological density dependent optical potential [8, 9, 11, 12] or a relativistic mean-field approach [12, 16, 17] yield strongly attractive K^- -nucleus potential of depths between 150–200 MeV. On the contrary, coupled-channel calculations using $\bar{K}N$ interaction adopted from chiral models and fitted to the low-energy $\bar{K}N$ scattering data [4] result in much shallower \bar{K} -nucleus potentials of depth $\sim 50 - 100$ MeV [16, 18, 19, 20].

The \bar{K} -nuclear interaction is strongly absorptive, which is due to one-nucleon absorption reactions $\bar{K}N \rightarrow \pi Y$ with approximately 100 MeV ($Y = \Sigma$) and 180 MeV ($Y = \Lambda$)

energy release for the final hyperon Y .

In recent years, the interest in this field has been focused on the question of possible existence of deeply bound \bar{K} -nuclear states. And sequentially, if such states exist, are they sufficiently narrow to allow identification in the experiment? These issues have attracted considerable interest recently when Kishimoto proposed to look for \bar{K} -nuclear states in in-flight (K^-, p) reactions [21]. Akaishi and Yamazaki suggested to search for $\bar{K}NN$ $I = 0$ state bound by over 100 MeV, for which the dominant $\bar{K}N \rightarrow \pi\Sigma$ decay channel would become kinematically forbidden [22, 23].

Following these suggestions some experimental evidence has been claimed for deeply bound K^- candidate states in (K^-_{stop}, n) and (K^-_{stop}, p) reactions on ^4He provided by the KEK-PS E471 experiment [24]. However, the peaks observed at KEK could be interpreted in terms of K^- absorption by a pair of nucleons [25]. Indeed, new revised experiment with better statistics have not confirmed the previously published results [26]. Interpretation in terms of \bar{K} -nuclear states was also used to explain few statistically weak irregularities measured in the in-flight (K^-, n) reactions on ^{16}O in the BNL-AGS parasite E930 experiment [27]. Other candidates for K^- -nuclear states were reported by the FINUDA collaboration in the K^-_{stop} reaction on $^6,^7\text{Li}$ and ^{12}C , detecting back-to-back Λp pairs coming from $K^-pp \rightarrow \Lambda p$ [28]. The FINUDA measurement suggested interpretation in terms of quasi-bound K^-pp clusters. However, this interpretation was again challenged in Refs. [29, 30].

The possible existence of deeply bound K^- -nuclear states was studied theoretically within various approaches. Unfortunately, calculations strongly depend on the applied model. As mentioned above, the fits to kaonic atom data, when extrapolated to the nuclear matter density yield a strongly attractive K^- -nucleus potential with the depth in the range 150–200 MeV. Consequently, these potentials support the idea of deeply bound K^- -nuclear states. Dynamical calculations of such states, taking into account polarization of the nuclear core due to strongly interacting K^- as well as reduction of phase space for the decay of the deeply bound K^- meson provide a lower limit of

$\Gamma_{K^-} \simeq 50$ MeV on the width of nuclear bound states for K^- binding energy in the range $B_{K^-} \sim 100 - 200$ MeV. On the other hand, models based on a chiral $\bar{K}N$ amplitude, giving much shallower optical potentials with the depth of 50–100 MeV, do not predict narrow deeply bound K^- states. The early calculations [31, 32] of few-body systems, which initiated the quest for K^- -nuclear states, did not use realistic $\bar{K}N$ and NN interaction. Very recent calculations based on Faddeev coupled-channel equations [33] give considerably larger widths than the above calculations of kaonic few-body systems.

As we have seen, the issue of deeply bound \bar{K} -nuclear states is still far from being understood. Clearly, the detailed treatment of ‘realistic’ $\bar{K}N$ interaction is needed when extrapolating to sub-threshold region. These extrapolations are still subject to uncertainties, which can be reduced by more accurate threshold data. Also the treatment of the NN interaction must be handled properly, since the short-range repulsion works against the strong compression of the nuclear core proposed in Ref. [31]. Finally, further studies of the multi-nucleonic absorption modes are essential, since these could substantially contribute to the widths of the K^- -nuclear states at the binding energies, where the dominant $\bar{K}N \rightarrow \pi\Sigma$ decay channel is kinematically forbidden.

In this paper, we present dynamical calculations of the K^- -nuclear states within the relativistic mean field (RMF) approach [34]. Following up previous works in this field [12, 35], our first aim was to explore in more detail the imaginary part of the optical potential in the energy region, where the dominant decay channel $\bar{K}N \rightarrow \pi\Sigma$ is closed. One such relevant modification has been done by incorporating the $\bar{K}N \rightarrow \pi\Lambda$ channel with threshold some 80 MeV below the $\pi\Sigma$ threshold. Further, we have considered the multinucleon absorption mode $\bar{K}NN \rightarrow YN$ to be ρ^2 density dependent. This is more appropriate for the description of the double-scattering nature of this process. The next goal of our calculations was to establish the effect of the p -wave interaction on the observables such as the K^- binding energy and width. Though the role of the $\bar{K}N$ p -wave interaction is marginal near threshold, it might become more important for antikaons deeply bound in the nuclear medium [36]. Finally, we studied more exotic

nuclear systems, containing more than one antikaon in order to examine the behavior of the nuclear medium under the influence of increasing strangeness.

In the next section we outline the \bar{K} -nucleus RMF methodology used in this work and describe our extension of the absorptive and p -wave interactions. The results are presented and discussed in Section 3 and in Section 4 we summarize the present work with conclusions and outlook.

2 Methodology

The K^- -nuclear states are studied using the theoretical framework of the relativistic mean-field (RMF) theory applied to a system of nucleons and K^- mesons. The interaction among hadrons is modeled through the exchange of scalar and several vector meson fields. The calculations are performed fully dynamically by successively allowing the K^- to polarize the nucleus and the polarized nucleus to affect the K^- -nuclear interaction.

The K^- -absorption modes are included within the optical model approach. The optical potential is constrained by the near-threshold K^- -atom data and follows the kinematical phase-space reduction for deeply bound K^- -nuclear states.

2.1 RMF model

Our starting point is a model of relativistic quantum field theory, proposed by Walecka and collaborators [37], which we have extended to incorporate (anti)kaonic sector. The nucleons (ψ) and (anti)kaons (K) are treated as Dirac and Klein–Gordon fields, respectively, interacting through the exchange of several meson fields.

The isoscalar-scalar σ -meson field is responsible for the attraction between all hadrons under consideration. The isoscalar-vector ω -meson field acts repulsively between nucleons as well as between antikaons but attractively between antikaons and nucleons. As a result the \bar{K} -nucleus interaction is strongly attractive in this approach.¹ The interaction of \bar{K} with the isovector-vector meson (ρ) plays a minor role and was not included in previous works (e.g. [12]). This is a good approximation for $N = Z$ nuclei, but not necessarily for the heavier ^{208}Pb nucleus. We note in this respect that optical potential fits for kaonic atoms, including data for nuclei with excess neutrons up to ^{238}U , found no need to

¹In contrary to the case of kaons, for which the vector field is repulsive and, as a result, the kaons in nuclear medium feel weak repulsion. This sign inversion of the vector interaction can be understood in terms of G -parity conjugation. [38]

introduce isovector components [10]. Since one of our aims is to investigate the behavior of multi- \bar{K} systems, we have introduced the ϕ -meson field. The ϕ -meson (“ $\phi = s\bar{s}$ ”) mediates the interaction exclusively between strange particles. Here we assume the ideal mixing of nucleons (i.e. no strange content) and follow the so-called OZI-rule, known from QCD, which, very roughly speaking, suppresses the interaction between quarks belonging to different generations [39]. Finally, the photon (A) accounts for the electromagnetic interaction. The π - and η -mesons with unnatural parity are not included because we are working with nuclear states which have well-defined parity. The model Lagrangian density then reads:

$$\begin{aligned}
\mathcal{L} = & \bar{\psi}(i\rlap{/}\partial - m_N)\psi \\
& + \frac{1}{2}\partial_\mu\sigma\partial^\mu\sigma - \frac{1}{2}m_\sigma^2\sigma^2 + g_{\sigma N}\bar{\psi}\psi\sigma + \frac{1}{3}g_2\sigma^3 - \frac{1}{4}g_3\sigma^4 \\
& - \frac{1}{4}\Omega_{\mu\nu}\Omega^{\mu\nu} + \frac{1}{2}m_\omega^2\omega_\mu\omega^\mu - g_{\omega N}\bar{\psi}\gamma_\mu\psi\omega^\mu + \frac{1}{4}d(\omega_\mu\omega^\mu)^2 \\
& - \frac{1}{4}\vec{R}_{\mu\nu}\cdot\vec{R}^{\mu\nu} + \frac{1}{2}m_\rho^2\vec{\rho}_\mu\cdot\vec{\rho}^\mu - g_{\rho N}\bar{\psi}\gamma_\mu\vec{\tau}\psi\cdot\vec{\rho}^\mu \\
& - \frac{1}{4}H_{\mu\nu}H^{\mu\nu} + \frac{1}{2}m_\phi^2\phi_\mu\phi^\mu \\
& - \frac{1}{4}F_{\mu\nu}F^{\mu\nu} - e\bar{\psi}\gamma_\mu\frac{1}{2}(1+\tau_3)\psi A^\mu \\
& + (\mathcal{D}_\mu\mathcal{K})^\dagger(\mathcal{D}^\mu\mathcal{K}) - m_K^2\mathcal{K}^\dagger\mathcal{K} + g_{\sigma K}m_K\mathcal{K}^\dagger\mathcal{K}\sigma,
\end{aligned} \tag{2.1}$$

where the kaon and nucleon fields are treated as iso-doublets:

$$\psi = \begin{pmatrix} \psi_p \\ \psi_n \end{pmatrix}, \quad \mathcal{K} = \begin{pmatrix} K \\ K^0 \end{pmatrix}. \tag{2.2}$$

The arrows above indicate isovector quantities, the dot denotes inner product, and $\vec{\tau}$ stands for the usual triplet of Pauli matrices. Moreover, m_N , m_σ , m_ω , m_ρ , m_ϕ and m_K are the nucleon, σ -, ω -, ρ -, ϕ - and K -meson masses, respectively. The $g_{\sigma N}$, $g_{\omega N}$, $g_{\rho N}$, e are coupling constants for the σ -, ω -, ρ -meson and the photon with respect to the nucleon, respectively, and $g_{\sigma K}$ is the σ -meson coupling constant for the (anti)kaon. The

field tensors for the vector mesons and the photon field in 2.1 are given by:

$$\begin{aligned}
\Omega_{\mu\nu} &\equiv \partial_\mu \omega_\nu - \partial_\nu \omega_\mu, \\
\vec{R}_{\mu\nu} &\equiv \partial_\mu \vec{\rho}_\nu - \partial_\nu \vec{\rho}_\mu - (g_{\rho N} + g_{\rho K}) \vec{\rho}_\mu \times \vec{\rho}_\nu, \\
H_{\mu\nu} &\equiv \partial_\mu \phi_\nu - \partial_\nu \phi_\mu, \\
F_{\mu\nu} &\equiv \partial_\mu A_\nu - \partial_\nu A_\mu.
\end{aligned} \tag{2.3}$$

The coupling of the (anti)kaon to the vector meson fields is introduced through the extended derivative \mathcal{D}_μ [40], which is defined as:

$$\mathcal{D}_\mu \equiv \partial_\mu + i g_{\omega K} \omega_\mu + i g_{\rho K} \vec{\tau} \cdot \vec{\rho}_\mu + i g_{\phi K} \phi_\mu + i e \frac{1}{2} (1 + \tau_3) A_\mu, \tag{2.4}$$

where $g_{\omega K}$, $g_{\rho K}$, $g_{\phi K}$ and e are the ω -, the ρ -, the ϕ -meson and the photon coupling constants with respect to the kaon.

Using the classical variational principle:

$$\delta \int d^4x \mathcal{L} [q_j(x), \partial_\mu q_j(x)] = 0 \Leftrightarrow \partial_\mu \left[\frac{\delta \mathcal{L}}{\delta (\partial_\mu q_j)} \right] - \frac{\delta \mathcal{L}}{\delta q_j} = 0, \tag{2.5}$$

where q_j is a generalized coordinate, $q_j \in \{\psi, \bar{\psi}, \mathcal{K}, \mathcal{K}^\dagger, \sigma, \omega_\mu, \vec{\rho}_\mu, \phi_\mu, A_\mu\}$, one obtains corresponding Euler–Lagrange equations of motion:

The Dirac equation for nucleons:

$$[i \not{\partial} - m_N + g_{\sigma N} \sigma - g_{\omega N} \gamma_\mu \omega^\mu - g_{\rho N} \gamma_\mu \vec{\tau} \cdot \vec{\rho}^\mu - e \gamma_\mu \frac{1}{2} (1 + \tau_3) A^\mu] \psi = 0, \tag{2.6}$$

the Klein–Gordon equation for the antikaon:

$$(\mathcal{D}_\mu^\dagger \mathcal{D}^\mu + m_K^2 - g_{\sigma K} m_K \sigma) \mathcal{K}^\dagger = 0, \tag{2.7}$$

and the meson fields:

$$\begin{aligned}
(\square + m_\sigma^2) \sigma &= g_{\sigma N} \bar{\psi} \psi + g_{\sigma K} m_K \mathcal{K}^\dagger \mathcal{K} + g_2 \sigma^2 - g_3 \sigma^3, \\
(\square + m_\omega^2) \omega_\mu &= g_{\omega N} \bar{\psi} \gamma_\mu \psi - g_{\omega K} \mathcal{K}^\dagger C_\mu^{(\omega)} \mathcal{K}, -d \omega_\mu (\omega_\nu \omega^\nu) \\
(\square + m_\rho^2) \vec{\rho}_\mu &= g_{\rho N} \bar{\psi} \gamma_\mu \vec{\tau} \psi - g_{\rho K} \mathcal{K}^\dagger \vec{\tau} C_\mu^{(\rho)} \mathcal{K} + (g_{\rho N} + g_{\rho K}) \vec{\rho}_\nu \times \vec{R}_{\mu\nu}, \\
(\square + m_\phi^2) \phi_\mu &= -g_{\phi K} \mathcal{K}^\dagger C_\mu^{(\phi)} \mathcal{K}, \\
\square A_\mu &= e \bar{\psi} \frac{1}{2} (1 + \tau_3) \gamma_\mu \psi - e \mathcal{K}^\dagger C_\mu^{(A)} \frac{1}{2} (1 + \tau_3) \mathcal{K},
\end{aligned} \tag{2.8}$$

where the common factor C_μ is defined as:

$$C_\mu^{(j)} = i \overleftrightarrow{\partial}_\mu + 2g_{jK} [g_{\omega K}\omega_\mu + g_{\rho K}\vec{\tau} \cdot \vec{\rho}_\mu + g_{\phi K}\phi_\mu + e \frac{1}{2}(1 + \tau_3)A_\mu] \quad (j = \omega, \rho, \phi, A). \quad (2.9)$$

We see that although the Dirac equation for nucleons (2.6) is not directly affected by the presence of antikaon the right hand sides of the equation of motion for the meson fields (2.8) contain (besides common nucleonic sources) the additional source terms induced by the antikaon. It is to be noted that in order to obtain the set of equations for the intermediate vector meson fields in the form (2.8), one must prove that the relation $\partial_\mu V^\mu = 0$ holds also for interacting fields. In Appendix B, we show that vector meson fields are coupled to the conserved (Noether) currents and hence $\partial_\mu V^\mu = 0$ is satisfied for our particular choice of the coupling scheme.

Equations (2.6)-(2.8) are non-linear quantum field equations and their exact solutions are very complicated. Moreover, since we expect coupling constants (except e) to be large, perturbative approaches are not useful. Fortunately, there exists approximative solution, which becomes increasingly valid as the nuclear density increases [37]. As the source terms on the r.h.s. of eq. (2.8) increase, the meson field operators can be replaced by their vacuum expectation values, which are classical fields.

Further, symmetries simplify the calculations considerably. We are looking for the nuclear ground states of doubly magic nuclei, and these are spherically symmetric. All the K^- mesons are assumed to occupy s -state, hence the spherical symmetry is retained. Rotational invariance implies, that space-like components of intermediate boson fields vanish. In this case, the meson fields and also the source terms on their r.h.s. depend only on the radial coordinate r . The electromagnetic charge conservation prohibits the charged components of the ρ -meson from appearing as classical fields. Finally, since we are looking for stationary states, the time-derivatives of the meson fields vanish. We can

then replace the meson fields by:

$$\begin{aligned}
\sigma(x) &\longrightarrow \langle \sigma(x) \rangle = \sigma(r) , \\
\omega_\mu(x) &\longrightarrow \langle \omega_\mu(x) \rangle = \delta_{\mu 0} \omega(r) , \\
\rho_\mu^i(x) &\longrightarrow \langle \rho_\mu^i(x) \rangle = \delta_{\mu 0} \delta^{i3} \rho(r) , \\
\phi_\mu(x) &\longrightarrow \langle \phi_\mu(x) \rangle = \delta_{\mu 0} \phi(r) , \\
A_\mu(x) &\longrightarrow \langle A_\mu(x) \rangle = \delta_{\mu 0} A(r) .
\end{aligned} \tag{2.10}$$

With these assumptions we can rewrite field equations (2.6)-(2.8) in the form:

$$\begin{aligned}
[-i\alpha_j \nabla_j + (m_N - g_{\sigma N} \sigma) \beta + g_{\omega N} \omega + g_{\rho N} \tau_3 \rho + e \frac{1}{2} (1 + \tau_3) A] \psi_i &= \varepsilon_i \psi_i , \\
(-\nabla^2 + m_\sigma^2) \sigma &= g_{\sigma N} \rho_s + g_2 \sigma^2 - g_3 \sigma^3 + g_{\sigma K} m_K \rho_{K^-}^{(s)} , \\
(-\nabla^2 + m_\omega^2) \omega &= g_{\omega N} \rho_v - g_{\omega K} \rho_{K^-} , \\
(-\nabla^2 + m_\rho^2) \rho &= g_{\rho N} \rho_3 - g_{\rho K} \rho_{K^-} , \\
(-\nabla^2 + m_\phi^2) \phi &= -g_{\phi K} \rho_{K^-} , \\
-\nabla^2 A &= e \rho_p - e \rho_{K^-} , \\
(-\nabla^2 + m_{K^-}^2 + \Pi_{K^-}) K^* &= E_{K^-}^2 K^* ,
\end{aligned} \tag{2.11}$$

where $\varepsilon_i = i \partial_t \psi_i$, $E_{K^-} = i \partial_t K^*$ and the antikaon self energy is given by:

$$\begin{aligned}
\text{Re } \Pi_{K^-} &= -g_{\sigma K} m_K \sigma - 2E_{K^-} (g_{\omega K} \omega + g_{\rho K} \rho + g_{\phi K} \phi + eA) \\
&\quad - (g_{\omega K} \omega + g_{\rho K} \rho - g_{\phi K} \phi + eA)^2 .
\end{aligned} \tag{2.12}$$

The source terms on the r.h.s. of (2.11) are defined as:

$$\begin{aligned}
\rho_s &= \langle : \bar{\psi} \psi : \rangle , \\
\rho_{K^-}^{(s)} &= K^* K , \\
\rho_v &= \langle : \psi^\dagger \psi : \rangle , & \int d^3x \rho_v &= A , \\
\rho_3 &= \langle : \psi^\dagger \tau_3 \psi : \rangle , & \int d^3x \rho_3 &= Z - N , \\
\rho_p &= \langle : \psi^\dagger \frac{1}{2} (1 + \tau_3) \psi : \rangle , & \int d^3x \rho_p &= Z , \\
\rho_{K^-} &= (E_{K^-} + g_{\omega K} \omega + g_{\rho K} \rho - g_{\phi K} \phi + eA_0) K^* K , & \int d^3x \rho_{K^-} &= \kappa ,
\end{aligned} \tag{2.13}$$

and the vector densities are normalized accordingly to yield proper (conserved) charges. The notation $\langle : \cdot : \rangle$ represents the vacuum expectation value of a normal ordered product of field operators. The vacuum is then represented by filled nucleon shells and κ negatively charged antikaons K^- . At this stage we are able to solve the equations (2.11) numerically. Details concerning the numerical solution can be found in Appendix C.

Finally, we derive the binding energy of the combined $\frac{A}{Z}X + \kappa K^-$ nuclear system:

$$B(A, Z, \kappa) = A m_N + \kappa m_K - E_{tot}, \quad (2.14)$$

where E_{tot} is the total energy of the system given by the vacuum expectation value of the Hamiltonian. The Hamiltonian is obtained by the Legendre dual transformation of the Lagrangian:

$$\begin{aligned} E_{tot} &= \langle : H : \rangle \\ &= \langle : p_i \dot{q}_i - L : \rangle \\ &= \int d^3x (\varepsilon_i \rho_v^{(i)} + E_{K^-} \rho_{K^-} - \langle : \mathcal{L} : \rangle) \\ &= \int d^3x \left\{ \frac{1}{2}[(\nabla\sigma)^2 + m_\sigma^2\sigma^2] - \frac{1}{2}[(\nabla\omega)^2 + m_\omega^2\omega^2] - \frac{1}{2}[(\nabla\rho)^2 + m_\rho^2\rho^2] \right. \\ &\quad - \frac{1}{2}[(\nabla\phi)^2 + m_\phi^2\phi^2] - \frac{1}{2}(\nabla A)^2 - \frac{1}{3}g_2\sigma^3 + \frac{1}{4}g_3\sigma^4 + \frac{1}{4}d\omega^4 \\ &\quad + \langle : \bar{\psi}_i[-i\nabla_j\gamma_j + m_N - g_{\sigma N}\sigma + g_{\omega N}\omega + g_{\rho N}\tau_3\rho + e\frac{1}{2}(1 + \tau_3)]\psi_i : \rangle \\ &\quad + (\nabla_j K^*)(\nabla_j K) + [m_K^2 - g_{\sigma K}m_K\sigma \\ &\quad \left. - (E_{K^-} + g_{\omega K}\omega + g_{\rho K}\rho + g_{\phi K}\phi + eA)^2]K^*K \right\}. \end{aligned} \quad (2.15)$$

The exponential decay of the meson fields at large distances permits the following partial integration:

$$\begin{aligned} \int d^3x \frac{1}{2}(\nabla\sigma)^2 + m_\sigma^2\sigma^2 &= \frac{1}{2} \int d^3x \sigma(-\nabla^2\sigma + m_\sigma^2\sigma) \\ &= \frac{1}{2} \int d^3x \sigma(g_{\sigma N} - g_2\sigma^2 + g_3\sigma^3 + g_{\sigma K}m_K K^* K). \end{aligned} \quad (2.16)$$

Similar manipulations for remaining fields, using the normalization conditions (2.13) and

Euler–Lagrange equations (2.11) lead to the final expression for the total binding energy:

$$\begin{aligned}
B(A, Z, \kappa) = & \sum_{i=1}^A (m_N - \varepsilon_i) + \kappa (m_K - E_{K^-}) \\
& - \frac{1}{2} \int d^3x (-g_{\sigma N} \sigma \rho_s + g_{\omega N} \omega \rho_v + g_{\rho N} \rho \rho_3 + e A \rho_p) \\
& - \frac{1}{2} \int d^3x (-\frac{1}{3} g_2 \sigma^3 - \frac{1}{2} g_3 \sigma^4 + \frac{1}{2} d \omega^4) \\
& + \frac{1}{2} \int d^3x [(g_{\omega K} \omega + g_{\rho K} \rho + g_{\phi K} \phi + e A) \rho_{K^-} + g_{\sigma K} m_K \sigma K^* K].
\end{aligned}$$

Then we can easily calculate the binding energy of the K^- :

$$B_{K^-} = B(A, Z, \kappa) - B(A, Z, \kappa - 1). \quad (2.17)$$

From the above expressions, it is evident that the K^- binding energy contains besides the single particle energies (with subtracted masses) also the additional mean-field contributions, which represent the rearrangement energy of the nuclear core.

2.2 Optical model phenomenology

As we have seen, the RMF approach can be naturally extended to incorporate antikaons in the nuclear medium. We are then able to calculate the K^- binding energy and estimate the dynamical response of the nuclear system to the presence of the K^- meson. Nevertheless, there are still important properties of K^- -nuclear states or phenomena of possible interest, which are not directly addressed by the traditional RMF methodology. One must then resort to more phenomenological models.

Imaginary potential

In order to achieve physical relevance of our calculations, we considered the K^- absorption modes in the nuclear medium, hence evaluated the decay width. In our model, the K^- -nuclear states acquire a width by allowing the antikaonic self energy Π_{K^-} to become complex and replacing $E_{K^-} \rightarrow E_{K^-} - i/2 \Gamma_{K^-}$. Since the imaginary part of the optical potential is not addressed by the RMF approach, the $\text{Im} \Pi_{K^-}$ was adopted from

the optical model phenomenology ². The optical potential depth was fitted to reproduce K^- atomic data, while the nuclear density was treated as a dynamical quantity in our selfconsistent calculations. Once the antikaon is embedded in the nuclear medium, the attractive $\bar{K}N$ interaction causes the rise of the nuclear density and thus leads to the increased \bar{K} width. On the other hand, the phase space available for decay products is reduced, especially in the case of deeply bound states. To render this, suppression factors multiplying $\text{Im } \Pi_{K^-}$ were introduced, explicitly considering \bar{K} binding energy for the initial decaying state and assuming two-body final state kinematics.

The first considered decay channel is the pionic conversion mode on a single nucleon:

$$\bar{K}N \rightarrow \pi\Sigma, \pi\Lambda \quad (70\%, 10\%), \quad (2.18)$$

with thresholds about 100 MeV and 180 MeV, respectively, below the $\bar{K}N$ total mass. Due to the single scattering nature of these processes, corresponding part of the pseudopotential is constructed in the first approximation:

$$\text{Im } \Pi_{K^-}^{(1)} = (0.7f_{1\Sigma} + 0.1f_{1\Lambda})V_0^{(1)}\rho_v(r), \quad (2.19)$$

where the factors 0.7 and 0.1 represent the branching ratios known from the CERN bubble chamber experiments [42], $V_0^{(1)}$ comes from the kaonic atom fits and the suppression factors f_{1Y} ($Y = \Sigma, \Lambda$) are given by:

$$f_{1Y} = \frac{M_{01}^3}{M_1^3} \sqrt{\frac{[M_1^2 - (m_\pi + m_Y)^2][M_1^2 - (m_Y - m_\pi)^2]}{[M_{01}^2 - (m_\pi + m_Y)^2][M_{01}^2 - (m_Y - m_\pi)^2}}} \Theta(M_1 - m_\pi - m_Y), \quad (2.20)$$

with $M_{01} = m_K + m_N$ and $M_1 = M_{01} - B_{K^-}$.

The second considered decay channel is the non-pionic conversion mode on two nucleons:

$$\bar{K}NN \rightarrow YN \quad (20\%), \quad (2.21)$$

with thresholds about $m_\pi \simeq 140$ MeV lower than the single-nucleon thresholds. Since this channel is heavily dominated by the ΣN final state, the ΛN channel was not

²See e.g. Ref. [41].

considered and our attention focused on the quadratic density dependence of the related part of the pseudopotential. The quadratic density dependence is a direct consequence of a double scattering character of the multinucleon absorption process, demanding usage of the second order term in the multiple scattering expansion for pseudopotential. The corresponding part of the pseudopotential in its double-scattering approximation is given by:

$$\text{Im } \Pi_{K^-}^{(2)} = 0.2 f_{2\Sigma} V_0^{(2)} \rho_v^2(r) / \rho_0, \quad (2.22)$$

where constant 0.2 represents branching ratio, $\rho_0 = 0.16 \text{ fm}^{-3}$ appears from dimensional requirements and $V_0^{(2)}$ is again determined from the kaonic atom data. The suppression factor $f_{1\Sigma}$ has the form:

$$f_{2\Sigma} = \frac{M_{02}^3}{M_2^3} \sqrt{\frac{[M_2^2 - (m_N + m_\Sigma)^2][M_2^2 - (m_\Sigma - m_N)^2]}{[M_{02}^2 - (m_N + m_\Sigma)^2][M_{02}^2 - (m_\Sigma - m_N)^2]} \Theta(M_2 - m_\Sigma - m_N), \quad (2.23)$$

with $M_{02} = m_K + 2m_N$ and $M_2 = M_{02} - B_{K^-}$.

***p*-wave interaction**

In addition to the *s*-wave interaction we considered also *p*-waves. Though the $\bar{K}N$ *p*-wave interaction, dominated by the $\Sigma(1385)$, plays only a minor role near threshold, it might become more important for the \bar{K} tightly bound in a nucleus [36]. In order to study the role of *p* waves, we have extended the K^- self energy Π_{K^-} to incorporate the *p*-wave interaction through the phenomenological Kisslinger potential [43]:

$$\Pi_{K^-}^{(P)} = 4\pi \left(1 + \frac{E_{K^-}}{m_N} \right)^{-1} [\nabla \rho_v(r)] \cdot c_0 \nabla, \quad (2.24)$$

where c_0 is due to the contribution of the $\Sigma(1385)$ *p*-wave resonance [44].

3 Results and discussion

We performed calculations of the K^- -nuclear s states in ^{12}C , ^{16}O , ^{40}Ca , and ^{208}Pb [34] using both the linear (L-HS [45]) and non-linear (NL-SH [46], NL-TM1(2) [47]) parametrizations of the nucleonic Lagrangian density. These RMF parametrizations give quite different predictions of the nuclear properties. In particular, the non-linear models yield in general a lower value of the nuclear compressibility³. Therefore, stronger polarization effects due to the presence of the K^- could be anticipated in comparison with the linear models.

The (anti)kaon coupling constants to the meson fields were chosen as follows: The coupling constant $g_{\omega K}^0$ was fixed to $g_{\omega K}^0 = 1/3g_{\omega N}$ following the simple quark model. The constant $g_{\sigma K}^0$ comes from the fits to kaonic atom data, which yielded $g_{\sigma K}^0 = 0.2g_{\sigma N}$ for linear and $g_{\sigma K}^0 = 0.233g_{\sigma N}$ for the non-linear parametrizations. Finally, the coupling constants $g_{\rho K}$ and $g_{\phi K}$ were adopted from $SU(3)$ relations: $2g_{\rho K} = \sqrt{2}g_{\phi K} = 6.04$ [40]. It is to be noted, that $g_{\sigma K}^0$ and $g_{\omega K}^0$ were taken as a ‘reference’ point of our calculations. In order to scan over different values of the K^- binding energies, a particular way of varying the coupling constants was used. Starting from $g_{iK} = \alpha_i g_{iK}^0 = 0$ ($i = \sigma, \omega$), we first scaled up $\alpha_\omega \rightarrow 1$. Then we scaled up $\alpha_\sigma \rightarrow 1$ (for $\alpha_\omega = 1$), and finally we again scaled up α_ω until the binding energy of $B_{K^-} \simeq 200$ MeV was reached.

3.1 Effects of additional meson fields

The coupling of the ρ -meson to the K^- acts repulsively on the K^- and produces a small decrease of the binding energy. Even for the case of ^{208}Pb , where the most significant effect can be anticipated due to large excess of neutrons, $N > Z$, the decrease of the value of B_{K^-} reaches $\lesssim 5$ MeV for $B_{K^-} \lesssim 200$ MeV for all the considered RMF parametrizations. More interesting is that the ρK^- coupling results in a weak isospin

³The compression modulus of nuclear matter is defined as: $K_\infty = 9\rho_0^2 \left. \frac{d^2 E}{d\rho^2} \right|_{\rho=\rho_0}$

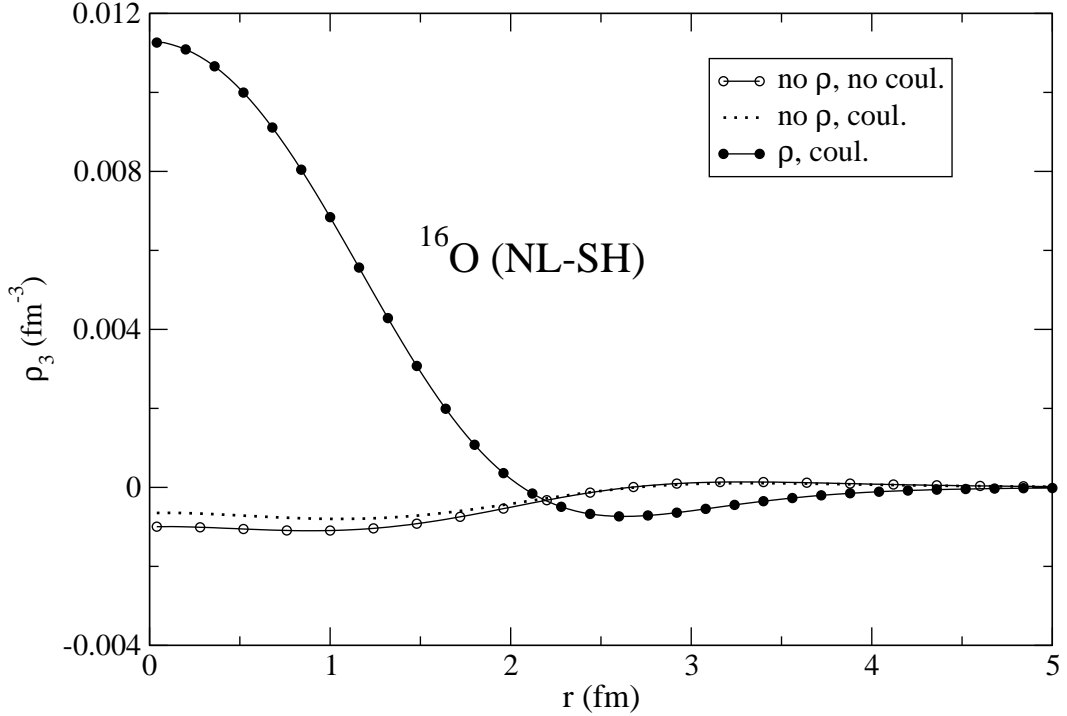


Figure 1: Isovector nuclear density $\rho_3 = \rho_p - \rho_n$ in $^{16}_{K^-}\text{O}$ with and without the interaction of K^- with the ρ -meson for the K^- binding energy $B_{K^-} = 100$ MeV, using the NL-SH parameter set.

deformation of the nuclear core. In Fig. 1 we show the effect of the ρK^- coupling on the isovector nuclear density ($\rho_3 = \rho_p - \rho_n$) in ^{16}O using the NL-SH parameter set. The open circles stand for the isovector nuclear density in the case when the K^- is bound by 100 MeV and does not interact via the ρ -meson and electromagnetic field. The dotted line then illustrates the modification of the isovector nuclear density when the K^- interacts electromagnetically but still not by the ρ -meson exchange. Finally, the solid circles represent the isovector nuclear density, when both the ρ -meson exchange and Coulomb interaction are switched on. The ρK^- coupling leads to additional rearrangement of the nuclear core. The proton density distribution is enhanced over the neutron distribution in the central part of the nuclear core. Note that the situation is inverse when the ρK^- coupling is not considered. This rearrangement is also apparent in the nucleonic single-particle energies presented in Fig. 2. First column shows the sequence of the

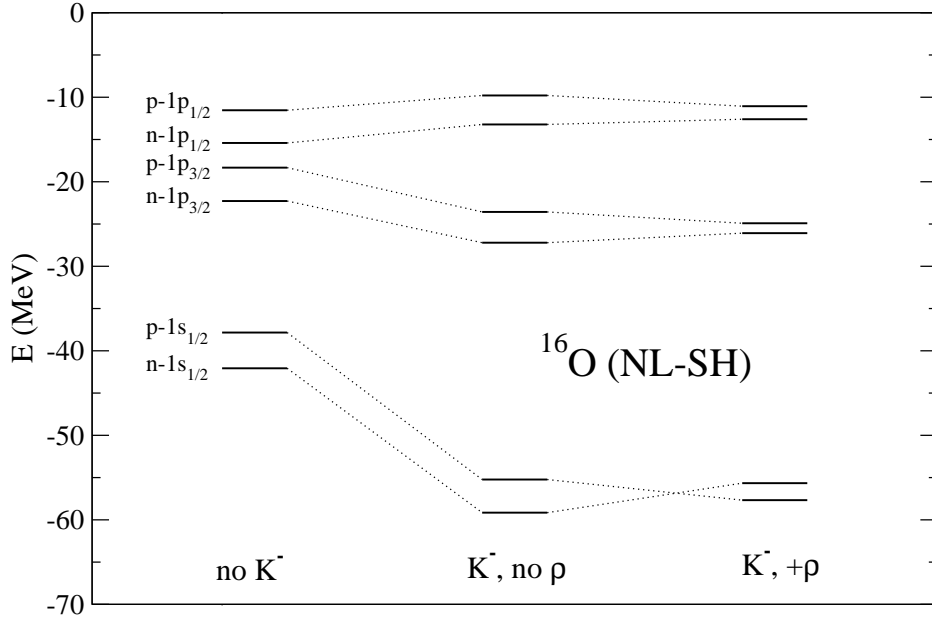


Figure 2: Nucleonic single-particle energies in ^{16}O with and without the interaction of K^- with the ρ -meson for $B_{K^-} = 100$ MeV, using NL-SH parameter set.

nucleon single-particle energies for ^{16}O in the absence of the K^- using the NL-SH model. The next column indicates the rearrangement of the single-particle energies produced by the K^- bound by 100 MeV, but with no ρK^- coupling. The last column displays further modification of the single-particle energies when ρK^- coupling is also considered. The most pronounced effect is observed for the $1s_{1/2}$ states, which become significantly more bound when the K^- is present. When the ρK^- coupling is included, the $1s_{1/2}$ proton and neutron energies change their order. Further, the energy splitting between the proton and neutron energy levels, caused by the Coulomb interaction, decreases since ρ -meson acts against the Coulomb interaction.

The addition of the ϕ -meson interaction produces a decrease of the K^- binding energy in systems with more than one K^- meson, as it mediates interaction exclusively among strange particles (see additional comments on Fig. 7). Generally, for all the considered parametrizations and nuclei the ϕ -repulsion increases with B_{K^-} due to the increasing source term (K^- density) on the r.h.s. of the equation of motion for the ϕ -meson field in (2.11) and amounts to several MeV for the binding energies $B_{K^-} \lesssim 200$ MeV.

3.2 Optical model modifications

In Fig. 3 we show the calculated width Γ_{K^-} as function of the binding energy B_{K^-} for $1s$ states in $^{12}_{K^-}\text{C}$ (upper panel) and $^{40}_{K^-}\text{Ca}$ (lower panel) for the nonlinear parameter set NL-SH. In the K^- absorption via the mesonic channel, we considered either only the $\pi\Sigma$

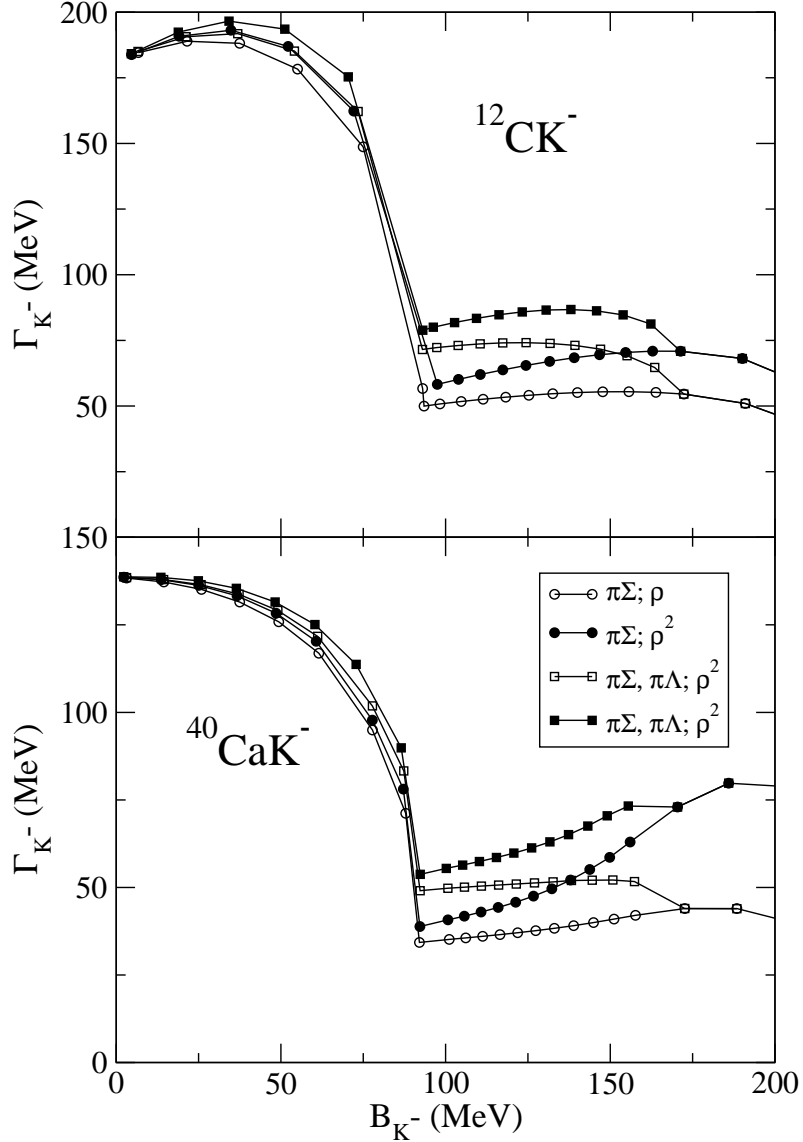


Figure 3: Widths of the $1s$ K^- -nuclear state in $^{12}_{K^-}\text{C}$ (upper panel) and $^{40}_{K^-}\text{Ca}$ (lower panel) as function of the K^- binding energy, for absorption through $\bar{K}N \rightarrow \pi\Sigma$ with or without $\bar{K}N \rightarrow \pi\Lambda$ and with ρ or ρ^2 dependence for $\bar{K}NN \rightarrow \Sigma N$ (for the NL-SH model).

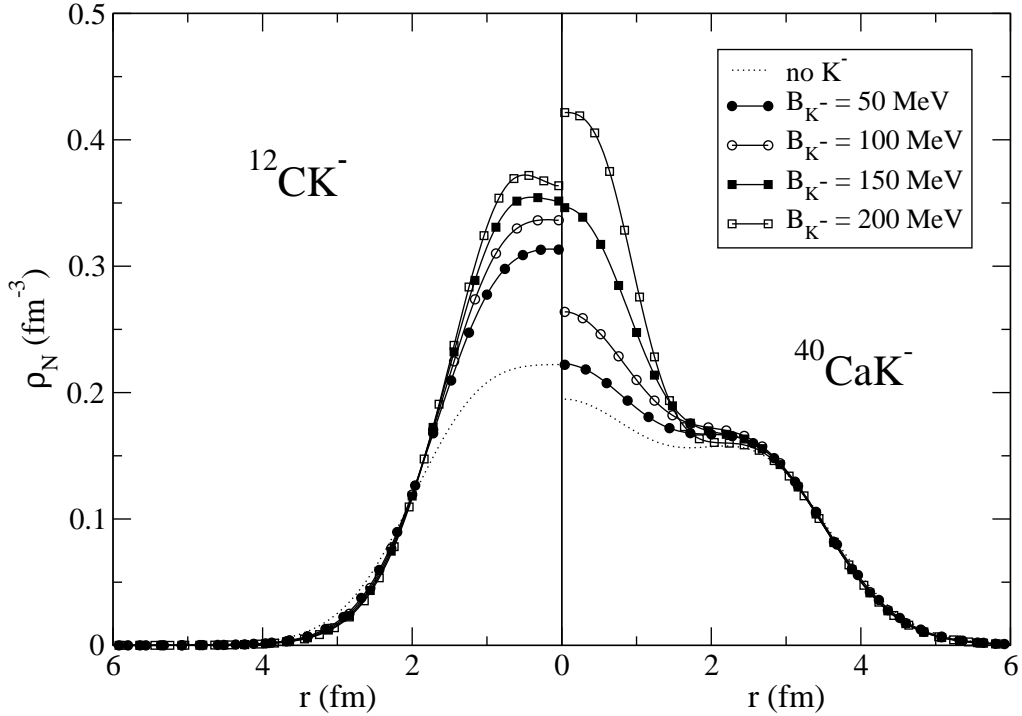


Figure 4: Nuclear density ρ_N of $^{12}_{K^-}\text{C}$ (left panel) and $^{40}_{K^-}\text{Ca}$ (right panel) for several $1s$ K^- -nuclear states with specified binding energy, for the NL-SH model. The dotted curves denote the corresponding nuclear density in the absence of the K^- meson.

mode (circles) or both the $\pi\Sigma$ and $\pi\Lambda$ decay modes (squares). The widths calculated assuming ρ and ρ^2 density dependence of the 2N-absorption mode are denoted by solid and empty symbols, respectively. Replacing ρ by ρ^2 for the density dependence of the multi-nucleon absorption of the K^- leads to increased widths of the $1s$ K^- -nuclear states as demonstrated in Fig. 3 for $^{12}_{K^-}\text{C}$ and $^{40}_{K^-}\text{Ca}$, and also in Fig. 5 and Fig. 6 for $^{16}_{K^-}\text{O}$ and $^{208}_{K^-}\text{Pb}$. The effect of the ρ^2 dependence of the 2N absorption mode clearly increases with the K^- binding energy B_{K^-} as a consequence of the increasing nuclear density. While it is less than 10 MeV for $B_{K^-} \lesssim 100$ MeV, for $B_{K^-} \gtrsim 150$ MeV it amounts to ≈ 20 MeV in carbon and even ≈ 30 MeV in calcium. It is to be noted that the increase of the width is particularly pronounced in ^{40}Ca for $B_{K^-} \gtrsim 150$ MeV. It is a consequence of much more pronounced increase of the central nuclear density in Ca than in C due to the strongly bound K^- , as demonstrated in Fig. 4.

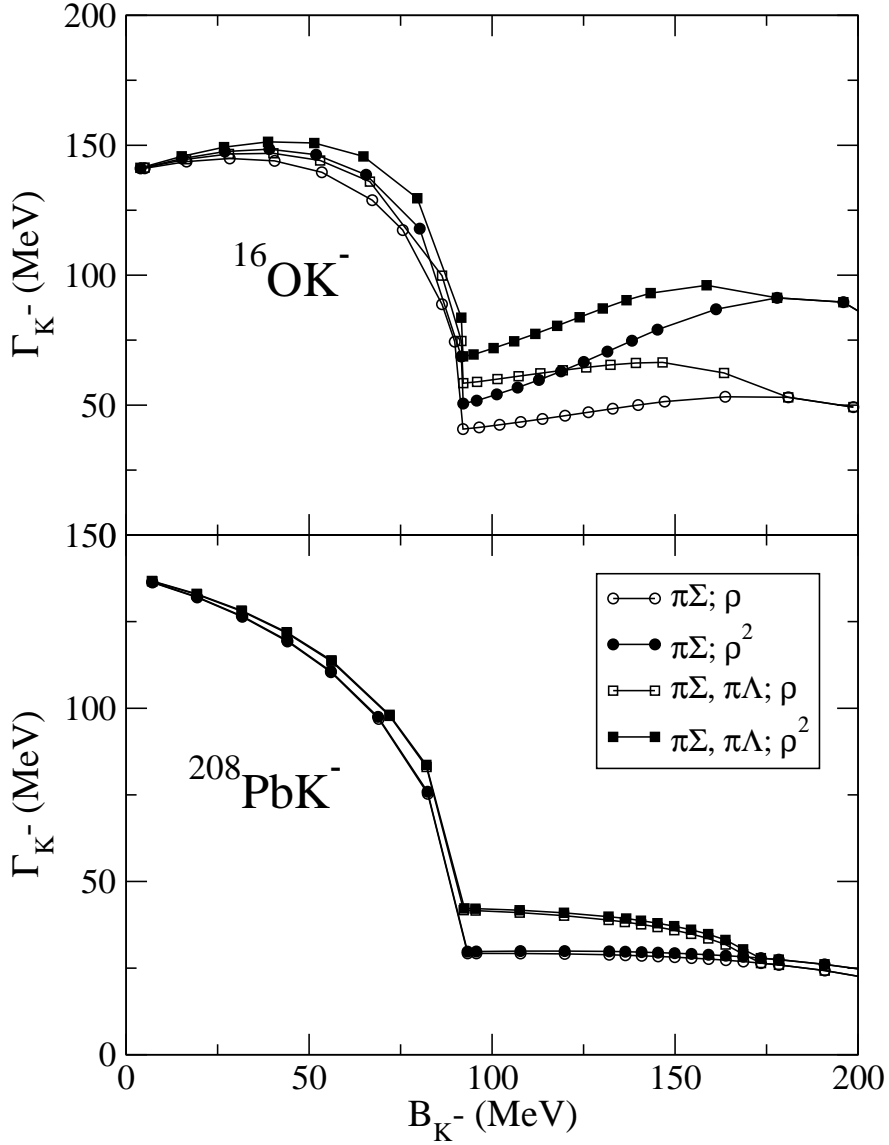


Figure 5: Widths of the $1s$ K^- -nuclear state in $^{16}_K\text{-O}$ for the NL-SH model (upper panel), and $^{208}_K\text{-Pb}$ for the L-HS model (lower panel) as function of the K^- binding energy.

For completeness, we present in Fig. 5 the widths Γ_{K^-} in ^{16}O for the nonlinear model NL-SH (upper panel) and in ^{208}Pb for the linear model L-HS (lower panel). Switching on the $\pi\Lambda$ adds further conversion width to K^- -nuclear states. In the energy range of $B_{K^-} \sim 100 - 160$ MeV, the width Γ_{K^-} increases by about 20 MeV. The $\pi\Lambda$ conversion vanishes at $B_{K^-} \approx 175$ MeV as illustrated in Figs. 3 and 5. The effect of the $\pi\Lambda$

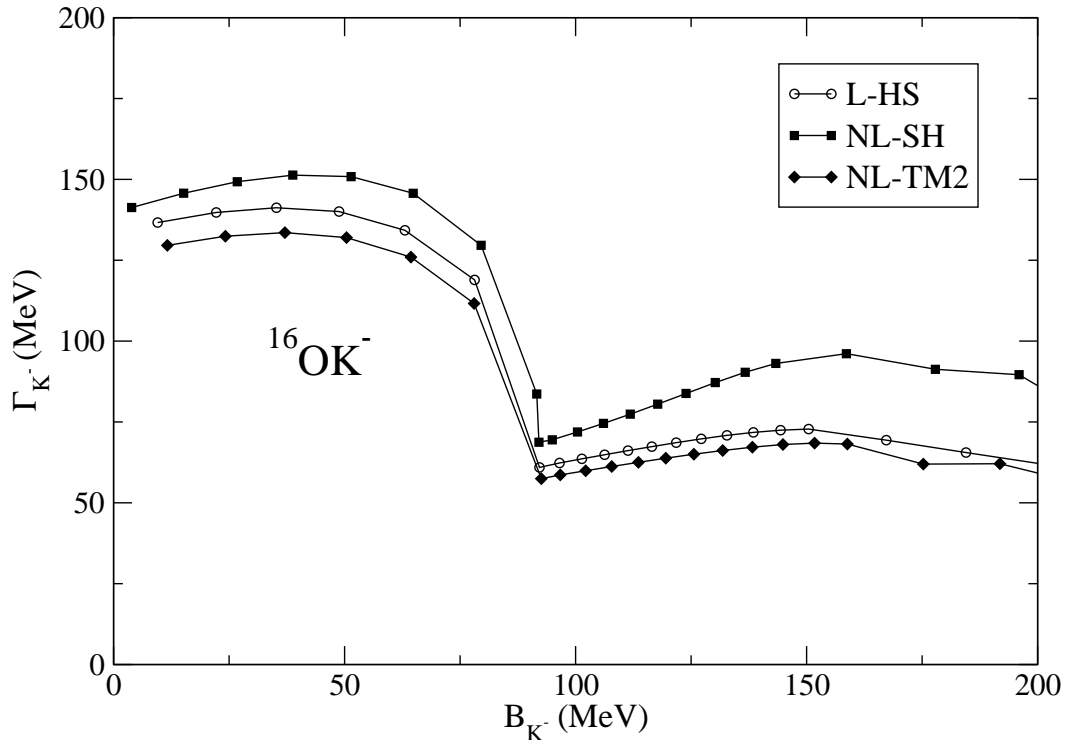


Figure 6: Widths of the $1s$ K^- -nuclear state in $^{16}_K\text{-O}$ as function of the K^- binding energy, for the L-HS, NL-SH and NL-TM2 parameter sets.

conversion is almost uniform for both linear and nonlinear parametrizations in all nuclei under consideration. On the other hand, the ρ^2 dependence of the multi-nucleon absorption mode exhibits strong sensitivity to the considered nucleus and also to the applied RMF model. In Pb, there is almost no difference between widths Γ_{K^-} calculated using the ρ and ρ^2 dependence. Nonlinear parametrizations, represented here by NL-SH and TM2, give larger increase of the decay width Γ_{K^-} due to the ρ^2 density dependence of the 2N absorption mode than linear ones as could be anticipated from lower compressibilities predicted by the nonlinear models. This model dependence is also illustrated in Fig. 6 on the widths Γ_{K^-} in ^{16}O calculated with the linear L-HS and nonlinear NL-SH and NL-TM2 parametrizations of the RMF model.

Finally, we studied the effect of the p -wave K^- -nucleus interaction. In Table 3.2 we show the effect of the p -wave interaction on the K^- binding energy B_{K^-} , single-particle binding energy $B_{K^-}^{sp}$ and decay width Γ_{K^-} for the $1s$ K^- -nuclear states. We present here

	^{12}C			^{40}Ca		
	B_{K^-} (MeV)	$B_{K^-}^{sp}$ (MeV)	Γ_{K^-} (MeV)	B_{K^-} (MeV)	$B_{K^-}^{sp}$ (MeV)	Γ_{K^-} (MeV)
S	100.0	109.8	51.1	100.0	104.4	35.0
S+P	112.8	123.3	56.9	105.6	111.8	38.3

Table 1: The effect of the p -wave interaction on the K^- binding energy B_{K^-} , single-particle binding energy $B_{K^-}^{sp} = m_K - \text{Re } E_{K^-}$ and decay width Γ_{K^-} for the $1s$ K^- -nuclear states in $^{12}_{K^-}\text{C}$ and $^{40}_{K^-}\text{Ca}$, for the NL-SH parameter set.

results just for a single value of the K^- binding energy, $B_{K^-} = 100$ MeV, and for the NL-SH parametrization. The corresponding values for the linear L-HS model are almost equivalent. In the Table, the results for only the s -wave K^- interaction are denoted by S while the calculations including the p -wave interaction are denoted by S+P. As can be seen, the introduction of the p -wave interaction leads to the increase of the binding energy by ≈ 12 MeV in $^{12}_{K^-}\text{C}$ and by ≈ 5 MeV in $^{40}_{K^-}\text{Ca}$. The decay width is then enhanced by ≈ 6 MeV for carbon and by ≈ 3 MeV for calcium. This enhancement of the decay width is a consequence of the dependence of the Γ_{K^-} on the K^- binding energy B_{K^-} in the relevant region of B_{K^-} (see Fig. 3) and also of the moderate increase of the nuclear density distributions when compared to the purely s -wave interaction.

3.3 Systems with more antikaons

In figure 7 we present $1s$ K^- binding energies B_{K^-} and widths Γ_{K^-} in ^{16}O with one and two bound antikaons for the NL-SH parameter set. The K^- binding energy B_{K^-} of the 2nd K^- in the double- K^- nucleus $^{16}_{2K^-}\text{O}$ is lower than the K^- binding energy in $^{16}_{1K^-}\text{O}$ for the binding energies B_{K^-} below $\lesssim 90$ MeV. Primarily, this is a consequence of the dominance of the mutual repulsion between the two K^- mesons over the polarization of the nuclear core caused by the presence of the second K^- . It is to be noted that this result is amplified by the larger width Γ_{K^-} in the case of two antikaons, which acts repulsively, and also by assuming just vector-meson exchanges at low binding energies

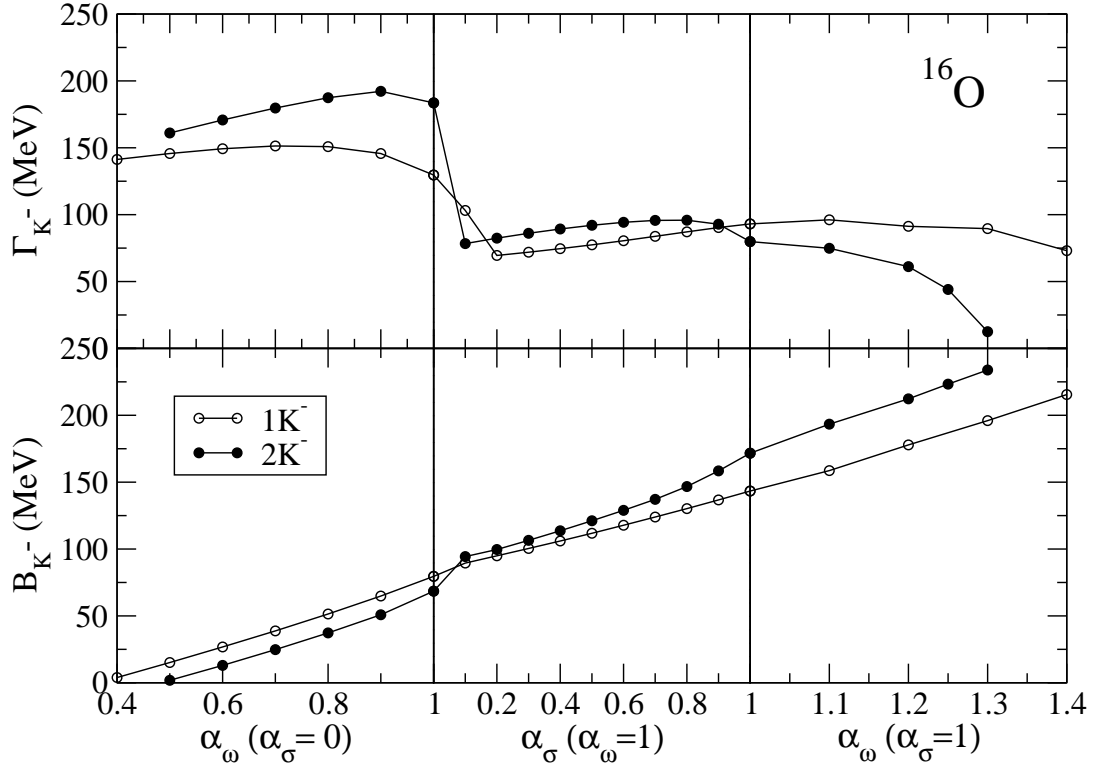


Figure 7: $1s$ K^- binding energy (upper panel) and width (lower panel) in ^{16}O with 1 and 2 antikaon(s) as function of the ωK and σK coupling strengths, for the NL-SH model (α_ω and α_σ are varied as indicated).

B_{K^-} , which are repulsive between K^- mesons (in contrast to the scalar interaction ⁴). The situation becomes inverse at $B_{K^-} \simeq 90$ MeV when the K^- binding energy in $^{16}_{2K^-}\text{O}$ becomes larger than in $^{16}_{1K^-}\text{O}$, reflecting strong polarization of the nuclear core (see fig. 8 and 9). The enhancement of the binding energy B_{K^-} in the double K^- nucleus is then responsible for the crossings of the curves for the K^- decay widths Γ_{K^-} at $B_{K^-} \simeq 90$ and 170 MeV, caused by the binding energy dependence of the suppression factor. We witness a sharp decrease of the width Γ_{K^-} in $^{16}_{2K^-}\text{O}$ at $B_{K^-} \simeq 230$ MeV, when the $2N$ -absorption channel of K^- gets closed.

⁴If we consider that antikaons interact solely via the (scalar) σ -meson exchange and switch off the imaginary potential, the binding energy B_{K^-} of the 2nd K^- in $^{16}_{2K^-}\text{O}$ is always larger than B_{K^-} in $^{16}_{1K^-}\text{O}$.

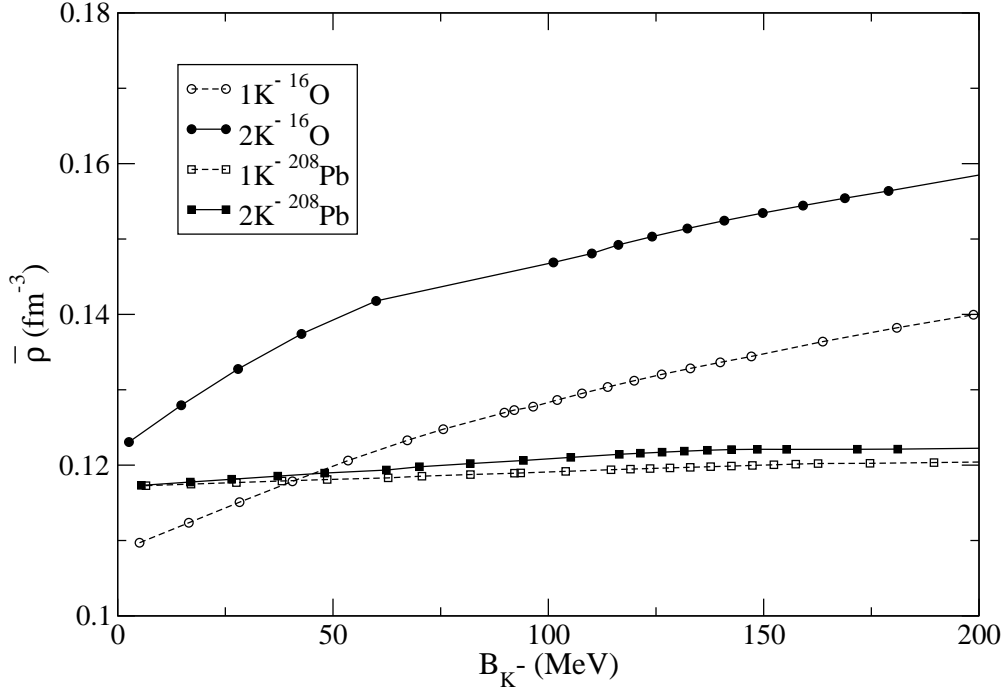


Figure 8: Average nuclear density $\bar{\rho}$ for ^{16}O and ^{208}Pb with $1K^-$ and $2K^-$'s as function of the $1s$ K^- binding energy, for the NL-SH model.

In figure 8 we show the average nuclear density $\bar{\rho}$ in ^{16}O and ^{208}Pb with one K^- meson and two K^- mesons as function of the K^- binding energy. Adding the second K^- to the nuclear system leads to further polarization of the nuclear core. The enhancement of the average nuclear density is quite pronounced in light nuclei (^{16}O) while in heavy nuclei (^{208}Pb) it is rather small.

The nuclear densities $\rho_N(r)$ and the K^- densities $\rho_{K^-}(r)$ due to one K^- and two K^- mesons embedded in the nuclear medium are compared in Fig. 9 for ^{16}O (top) and ^{208}Pb (bottom). The presented density distributions correspond to various selected values of B_{K^-} , as indicated. For comparison, we also show the density distribution ρ_N for the nucleus without K^- . The K^- density ρ_{K^-} is normalized to the number of antikaons κ in the system. The ρ_{K^-} distributions indicate that the antikaons in the s-state are concentrated near the nuclear center. This causes a sizable enhancement of the nuclear density $\rho_N(r)$ in the neighboring region, strongly localized within $r \leq 2$ fm. This is particularly distinct in the case of Pb for higher values of B_{K^-} .

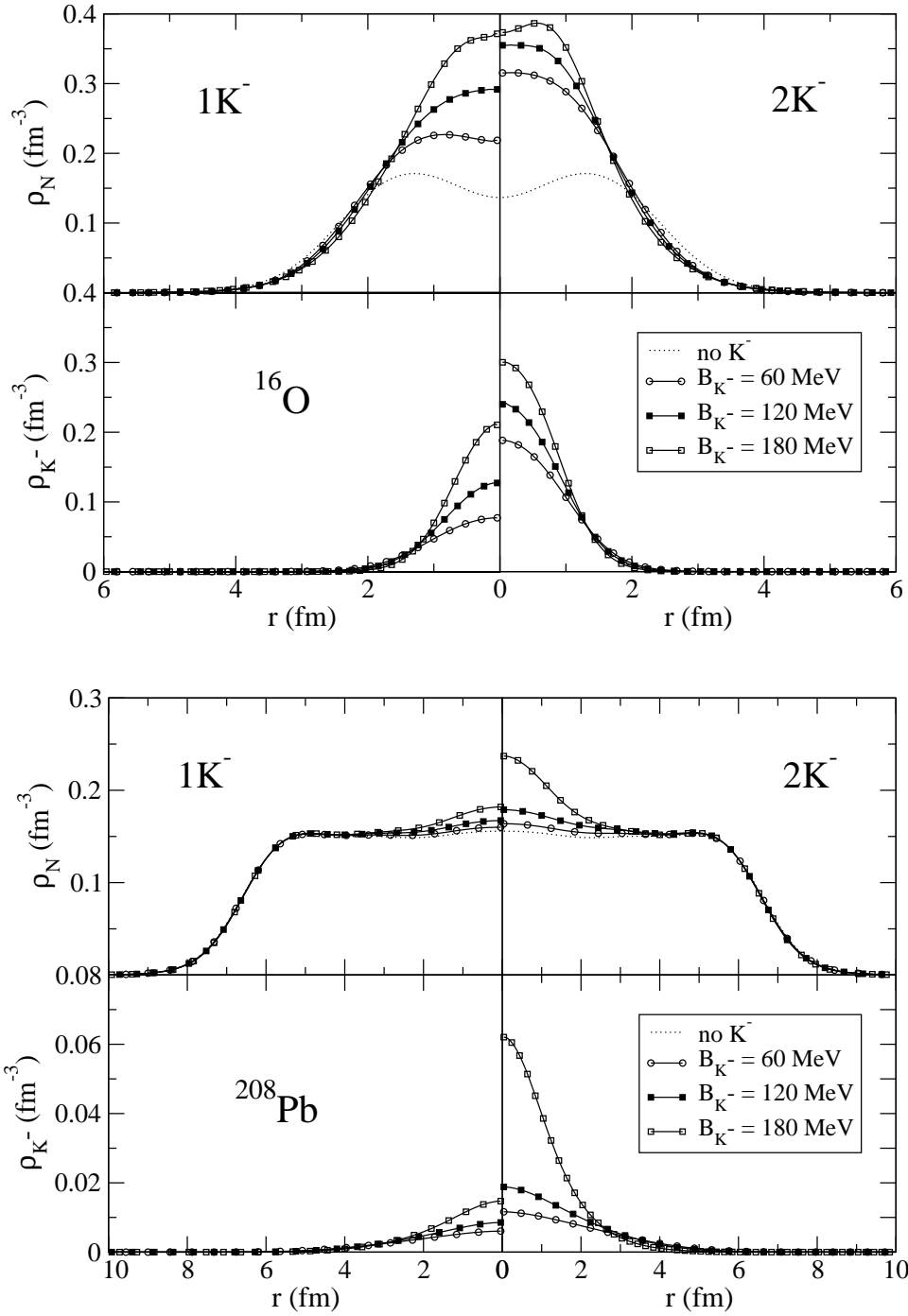


Figure 9: Nuclear density ρ_N (top) and K^- density ρ_{K^-} (bottom) in ^{16}O with 1 K^- (left) and 2 K^- 's (right), for the NL-SH model. The dotted curve stands for the ^{16}O density in the absence of the K^- meson.

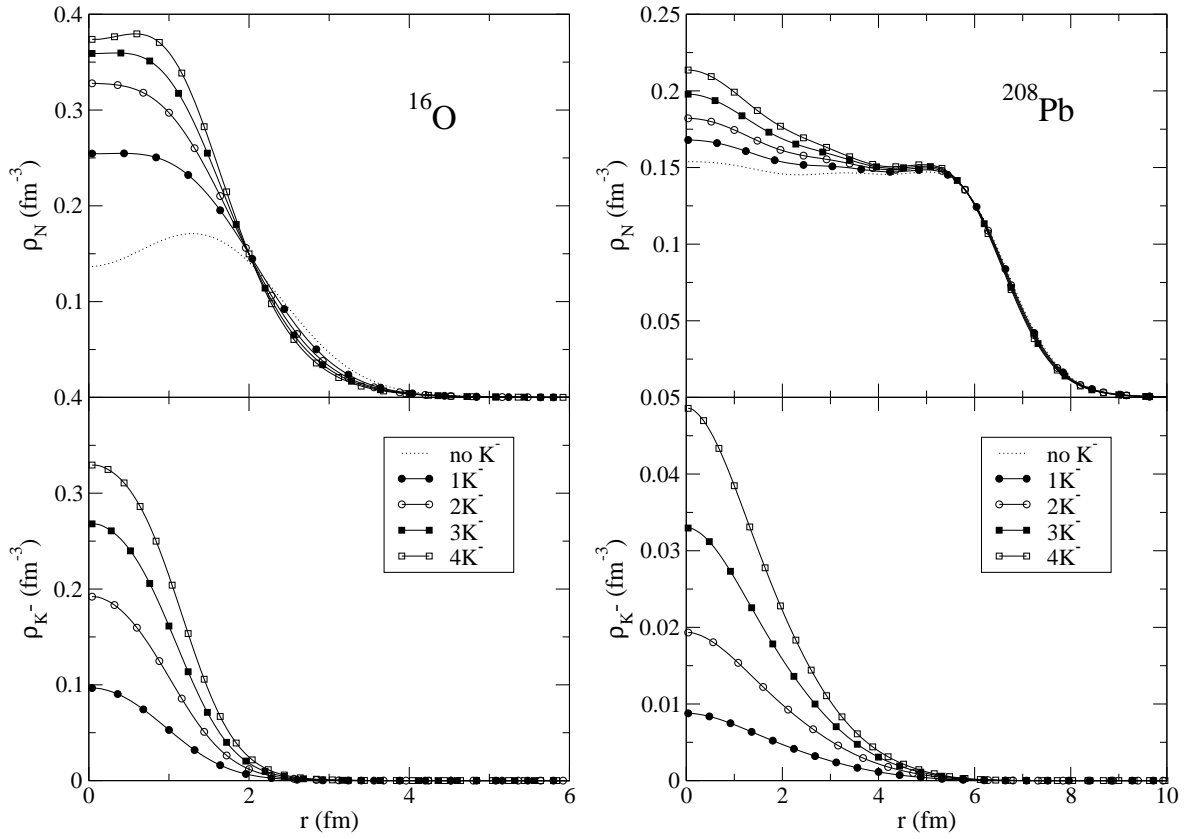


Figure 10: Nuclear density ρ_N (upper panels) and K^- density ρ_{K^-} (lower panels) in ^{16}O and ^{208}Pb with 1, 2, 3 and 4 antikaons, for the NL-SH model. The last K^- is bound by $B_{K^-} = 100$ MeV. The dotted curve stands for the ^{16}O density in the absence of the K^- meson.

In Fig. 10 we present density distributions ρ_N and ρ_{K^-} in ^{16}O and ^{208}Pb with 1,2,3, and 4 antikaons calculated within the NL-SH parametrization. The K^- couplings were chosen such that the last K^- was bound by 100 MeV. The K^- density is again normalized to the number of antikaons κ . The density distributions behave quite regularly as function of κ ; we witness gradual increase of ρ_{K^-} . The central nuclear density in $^{16}_{4K^-}\text{O}$, with a small saddle at $r \approx 0$, is only about 50% larger than ρ_N in $^{16}_{1K^-}\text{O}$. In ^{208}Pb , the central nuclear density for $\kappa = 4$ is enhanced even less, by about 30% compared to the nucleus with one K^- meson embedded.

4 Summary

In the present work, we analyzed in detail processes and conditions, which determine the decay width of deeply bound K^- -nuclear states in the nuclear medium. We performed fully selfconsistent dynamical calculations of the K^- -nuclear states within the RMF approach. In our calculations we allowed for a few K^- mesons to be embedded in the nuclear medium.

We verified that the interaction of the K^- meson with the ρ -meson field has a small effect on the K^- binding energy and produces weak isospin deformation of the nuclear core. For all considered nuclei and RMF parametrizations the ρ -meson exchange decreases the K^- binding energy B_{K^-} by $\lesssim 5$ MeV for $B_{K^-} \lesssim 200$ MeV. Similarly, the introduction of the ϕ -meson exchange in systems with more K^- mesons leads to a decrease of the K^- binding energy by several MeV in the considered range of B_{K^-} .

The introduction of the $\pi\Lambda$ decay channel in the single-nucleon absorption mode enhances the K^- conversion width for the K^- binding energies $B_{K^-} \lesssim 170$ MeV. This enhancement is almost uniform for both linear and nonlinear parametrizations in all nuclei under consideration. The most remarkable contribution occurs for the K^- binding energies in the range $B_{K^-} \approx 100 - 160$ MeV and reaches ≈ 20 MeV. The assumption of the ρ^2 density dependence for the $2N$ -absorption mode adds further conversion width especially to the deeply bound K^- -nuclear states. The increase is particularly large for lighter nuclei and nonlinear parametrizations as anticipated from strong polarization effects.

We studied nuclear systems containing a few K^- mesons. The calculations revealed that the K^- and nuclear densities behave quite regularly with increasing number of antikaons embedded in the nuclear medium. The central nuclear density in ${}^{16}_{4K}\text{O}$ and ${}^{208}_{4K}\text{Pb}$ is only about 50% and 30%, respectively, larger than the central nuclear densities in systems with one K^- meson.

The calculations involving the p -wave interaction of the K^- meson with a nucleus

indicate that the p -wave interaction plays only a minor role in heavier nuclear systems. Since the influence of the p -wave interaction increases with the decreasing atomic number, it may still become important for tightly bound few-body K^- systems.

References

- [1] B.D. Kaplan and A.E. Nelson, Phys. Lett. **175** (1986) 57.
- [2] A.E. Nelson, B.D. Kaplan, Phys. Lett. B **192** (1987) 193.
- [3] R.H. Dalitz, T.C. Wong, G. Rajasekaran, Phys. Rev. **153** (1967) 1617.
- [4] A.D. Martin, Nucl. Phys. B **179** (1981) 33.
- [5] M. Iwasaki *et al.*, Phys. Rev. Lett. **78** (1997) 3067; T.M. Ito *et al.*, Phys. Rev. C **58** (1998) 2366.
- [6] A. Müller-Groeling, K. Holinde, J. Speth, Nucl. Phys. A **513** (1990) 557.
- [7] T. Waas, N. Kaiser, W. Weise, Phys. Lett. B **365** (1996) 12; Phys. Lett. B **379** (1996) 34; N. Kaiser, P.B. Siegel, W. Weise, Nucl. Phys. A **594** (1995) 325; W. Weise, Nucl. Phys. A **610** (1996) 35.
- [8] E. Friedman, A. Gal, C.J. Batty, Phys. Lett. B **308** (1993) 6.
- [9] E. Friedman, A. Gal, C.J. Batty, Nucl. Phys. A **579** (1994) 518.
- [10] C.J. Batty, E. Friedman, A. Gal, Phys. Rep. **287** (1997) 385. 518.
- [11] E. Friedman, A. Gal, J. Mareš, A. Cieplý, Phys. Rev. C **60** (1999) 024314.
- [12] J. Mareš, E. Friedman, A. Gal, Nucl. Phys. A **770** (2006) 84.
- [13] F. Laue *et al.*, Phys. Rev. Lett. **82** (1999) 1640.
- [14] F. Laue *et al.*, Eur. Phys. J. A **9** (2000) 397.
- [15] M. Menzel *et al.*, Phys. Lett. B **495** (2000) 26.
- [16] G.E. Brown, M. Rho, Nucl. Phys. A **596** (1996) 503.
- [17] E. Friedman, A. Gal, J. Mareš, A. Cieplý, Phys. Rev. C **60** (1999) 024314.

- [18] T. Waas, N. Kaiser, W. Weise, Phys. Lett. B **379** (1996) 34.
- [19] J. Shaffner-Bielich, V. Koch, M. Effenberger, Nucl. Phys. A **669** (2000) 153; A. Ramos, E. Oset, Nucl. Phys. A **671** (2000) 481; A. Cieplý, E. Friedman, A. Gal, J. Mareš, Nucl. Phys. A **696** (2001) 173.
- [20] A. Baca, C. García-Recio, J. Nieves, Nucl. Phys. A **673** (2000) 335.
- [21] T. Kishimoto, Phys Rev. Lett. B **83** (1999) 4701.
- [22] Y. Akaishi, T. Yamazaki, in *Proc. DAΦNE Workshop*, Frascati Physics Series XVI (1999) 59; Phys. Rev. C **65** (2002) 044005.
- [23] T. Yamazaki, Y. Akaishi, Phys. Lett. B **535** (2002) 70.
- [24] M. Iwasaki, *et al.*, nucl-ex/0310018; T. Suzuki, *et al.*, Nucl. Phys. A **754** (2005) 375c.
- [25] E. Oset, H. Toki, Phys. Rev. C **74** (2006) 01527.
- [26] T. Suzuki, *et al.*, Phys. Lett. B **597** (2004) 263.
- [27] T. Kishimoto, *et al.*, Nucl. Phys. A **754** (2005) 383c.
- [28] M. Agnello *et al.*, Phys Rev. Lett. **94** (2005) 212303.
- [29] J. Mareš, E. Friedman, A. Gal, Phys. Rev. Lett. B **606** (2005) 295; Nucl. Phys. A **770** (2006) 84.
- [30] V.K. Magas, E. Oset, A. Ramos, H. Toki, Phys. Rev. C **74** (2006) 025206.
- [31] Y. Akaishi, T. Yamazaki, in *Frascati Physics Series Vol. XVI, Proc. III Int. Workshop on Physics and Detectors for DAΦNE*, eds. S. Bianconi *et al.* (LNF, Frascati, 1999) p. 59; Phys. Rev. C **65** (2002) 044005.
- [32] A. Doté, H. Horiuchi, Y. Akaishi, T. Yamazaki, Phys. Lett. B **590** (2004) 51; Phys. Rev. C **70** (2004) 044313.

- [33] N.V. Shevchenko, A. Gal, J. Mareš, Phys. Rev. Lett. **98** (2007) 082301.
- [34] D.Gazda, E. Friedman, A. Gal, J. Mareš, to be published.
- [35] D. Gazda, Research project, CTU Prague (2006).
- [36] S. Wycech, A.M. Green, arXiv:nucl-th/0501019v1.
- [37] B.D. Serot, J.D. Walecka, Adv. Nucl. Phys. **16** (1986) 1.
- [38] W. Greiner, Quantum Mechanics: Symmetries, Springer-Verlag Berlin Heidelberg, Germany (1989).
- [39] B.K. Jennings, Phys. Lett. B **246** (1990) 325.
- [40] J. Schaffner, I.N. Mishustin, Phys. Rev. C **53** (1996) 1416.
- [41] M.L. Goldberger, K.M. Watson, Collision theory, John Wiley & Sons, Inc., New York (1964).
- [42] C. Vander Velde-Wilquet, J. Sacton, J.H. Wickens, D.N. Tovee, D.H. Davis, Nuovo Cimento A **39** (1977) 538.
- [43] L.S. Kisslinger, Phys. Rev. **98** (1955) 761.
- [44] W. Weise, arXiv:nucl-th/0701035v1.
- [45] C.J. Horowitz, B.D. Serot, Nucl. Phys. A **368** (1981) 503.
- [46] M.M. Sharma, M.A. Nagarajan, P. Ring, Phys. Lett. B **312** (1993) 377.
- [47] Y. Sugahara, H. Toki, Nucl. Phys. A **579** (1994) 557.
- [48] J.D. Björken, S.D. Drell, Relativistic Quantum Mechanics, McGraw-Hill, New York, 1964.

Appendices

A Notation and conventions

We adhere primarily to the conventions of Bjorken and Drell [48]. Physical units are chosen with $\hbar = c = 1$.

Contravariant x^μ and covariant x_μ four-vectors are written as:

$$\begin{aligned}x^\mu &= (t, \vec{x}) \equiv x, \\x_\mu &= (t, -\vec{x}), \\ \partial^\mu &\equiv \frac{\partial}{\partial x_\mu} = \left(\frac{\partial}{\partial t}, -\nabla \right), \\ \partial_\mu &\equiv \frac{\partial}{\partial x^\mu} = \left(\frac{\partial}{\partial t}, \nabla \right).\end{aligned}\tag{A.1}$$

The Dirac equation for a free particle of mass M reads:

$$(i\gamma_\mu \partial^\mu - M)\psi = (i\rlap{/}\partial - M)\psi = 0,\tag{A.2}$$

where we use Feynman “slash” notation $\rlap{/}\partial \equiv a_\mu \gamma^\mu$. The gamma matrices obey:

$$\gamma^\mu \gamma^\nu + \gamma^\nu \gamma^\mu = \{\gamma^\mu, \gamma^\nu\} = 2g^{\mu\nu},\tag{A.3}$$

where $g^{\mu\nu}$ is a metric tensor given by:

$$g^{\mu\nu} = \text{Diag}(1, -1, -1, -1, -1).\tag{A.4}$$

In the standard (Dirac-Pauli) realization the gamma matrices are written as:

$$\gamma^0 = \begin{pmatrix} \mathbb{1} & 0 \\ 0 & -\mathbb{1} \end{pmatrix}, \quad \vec{\gamma} = \begin{pmatrix} \vec{\sigma} & 0 \\ 0 & -\vec{\sigma} \end{pmatrix},\tag{A.5}$$

with the Pauli matrices defined by:

$$\sigma_1 = \begin{pmatrix} 0 & 1 \\ 1 & 0 \end{pmatrix}, \quad \sigma_2 = \begin{pmatrix} 0 & -i \\ i & 0 \end{pmatrix}, \quad \sigma_3 = \begin{pmatrix} 1 & 0 \\ 0 & -1 \end{pmatrix}.\tag{A.6}$$

B Conserved currents

The existence of conserved currents is a direct consequence of the invariance of the Lagrangian density (2.1) under the global transformations of the involved fields. Using Euler–Lagrange equations (2.5), it follows that:

$$\begin{aligned} 0 \equiv \delta \mathcal{L} &= \frac{\delta \mathcal{L}}{\delta q_j} \delta q_j + \frac{\delta \mathcal{L}}{\delta (\partial_\mu q_j)} \delta (\partial_\mu q_j) \\ &= \partial_\mu \left(\frac{\delta \mathcal{L}}{\delta (\partial_\mu q_j)} \delta q_j \right) = \partial_\mu j^\mu \end{aligned} \quad (\text{B.1})$$

It is then straightforward, using Gauss–Ostrogradski–Green theorem, to show that:

$$\frac{dF}{dt} \equiv \frac{d}{dt} \int d^3x j^0(x) = 0, \quad (\text{B.2})$$

i.e., F represents a conserved quantity (charge).

At first we consider the global phase transformation of the nucleonic and kaonic isospinors:

$$\psi \rightarrow e^{i\lambda_N} \psi, \quad \mathcal{K} \rightarrow e^{i\lambda_K} \mathcal{K}, \quad (\text{B.3})$$

where $\lambda_N, \lambda_K \in \mathbb{R}$. The Lagrangian density (2.1) is evidently invariant under this transformation. Using (B.3) and expanding transformed fields for $\lambda_N, \lambda_K \rightarrow 0$, we obtain field variations:

$$\begin{aligned} e^{i\lambda_N} \psi &\simeq (1 + i\lambda_N) \psi \quad \Rightarrow \quad \delta \psi = i\lambda_N \psi, \\ e^{i\lambda_K} \mathcal{K} &\simeq (1 + i\lambda_K) \mathcal{K} \quad \Rightarrow \quad \delta \mathcal{K} = i\lambda_K \mathcal{K}, \end{aligned} \quad (\text{B.4})$$

Following (B.1) one obtains conserved current induced by this symmetry transformation:

$$\begin{aligned} j_v^\mu &= \lambda_N \bar{\psi} \gamma^\mu \psi \\ &+ \lambda_K \mathcal{K}^\dagger \{ i \overleftrightarrow{\partial}_\mu + 2g_{\omega K} [g_{\omega K} \omega_\mu + g_{\rho K} \vec{\tau} \cdot \vec{\rho}_\mu + g_{\phi K} \phi_\mu + e \frac{1}{2} (1 + \tau_3) A_\mu] \} \mathcal{K}. \end{aligned} \quad (\text{B.5})$$

The first part of j_v^μ can be identified with the baryonic current, thus the conserved quantity (B.2) is the baryon number. The second part, connected to the kaon field, leads to the conservation of the kaon number.

The next transformation which clearly leaves the Lagrangian density invariant is the same transformation as (B.3) but realized only on the upper components of the kaon and nucleon isospinors:

$$\psi_p \rightarrow e^{i\lambda_N} \psi_p, \quad K \rightarrow e^{i\lambda_K} K. \quad (\text{B.6})$$

By similar manipulations as in the previous case we again get the field variations:

$$\delta\psi_p = i\lambda_N\psi_p \quad \delta K = i\lambda_K K, \quad (\text{B.7})$$

which by substituting into (B.1) lead to the following current:

$$j_e^\mu = \lambda_N \bar{\psi} \gamma^\mu \frac{1}{2} (1 + \tau_3) \psi + \lambda_K \mathcal{K}^\dagger \frac{1}{2} (1 + \tau_3) \left\{ i \overleftrightarrow{\partial}_\mu + 2g_{\omega K} [g_{\omega K} \omega_\mu + g_{\rho K} \vec{\tau} \cdot \vec{\rho}_\mu + g_{\phi K} \phi_\mu + e \frac{1}{2} (1 + \tau_3) A_\mu] \right\} \mathcal{K}, \quad (\text{B.8})$$

which can be interpreted as the electromagnetic current and leads to the conservation of the electromagnetic charge.

The last conserved current, which we need for derivation of the equations of motion for the meson fields in (2.8), is induced by the isospin transformation:

$$\psi \rightarrow e^{i\vec{\theta} \cdot \vec{\tau}} \psi, \quad \mathcal{K} \rightarrow e^{i\vec{\theta} \cdot \vec{\tau}} \mathcal{K}, \quad \vec{\rho}_\mu \rightarrow e^{i\vec{\theta} \cdot \vec{T}} \vec{\rho}_\mu, \quad (\text{B.9})$$

where $\vec{\theta} \in \mathbb{R}^3$ may differ for each field, which is not indicated here for simplicity of the following formulae.

It is not immediately evident, that this transformation leaves the Lagrangian density invariant. We can restrict ourselves to the infinitesimal transformations:

$$\begin{aligned} \psi &\rightarrow (1 + i\vec{\theta} \cdot \vec{\tau}) \psi, \\ \mathcal{K} &\rightarrow (1 + i\vec{\theta} \cdot \vec{\tau}) \mathcal{K}, \\ \rho_\mu^j &\rightarrow (1 + i\theta_i (T_i)_{jk}) \rho_\mu^k = [1 + i\theta_i (-i\varepsilon_{ijk})] \rho_\mu^k \\ &= (\vec{\rho}_\mu + \vec{\theta} \times \vec{\rho}_\mu)^j, \end{aligned} \quad (\text{B.10})$$

since every finite transformation can be obtained as infinite set of infinitesimal transformations. Next we can show, that the isospin transformation preserves squares of the following quantities:

- $\bar{\psi}\tau_j\psi \rightarrow (\bar{\psi} - i\bar{\psi}\theta_i\tau_i)\tau_j(\psi + i\theta_i\tau_i\psi) = \bar{\psi}\tau_j\psi + i\bar{\psi}\tau_j\theta_i\tau_i\psi - i\bar{\psi}\theta_i\tau_i\tau_j\psi + \mathcal{O}(\theta^2)$
 $\simeq \bar{\psi}\tau_j\psi + i\bar{\psi}\theta_i[\tau_j, \tau_i]\psi = \bar{\psi}\tau_j\psi + i\bar{\psi}\theta_i(2i\varepsilon_{jik}\tau_k)\psi = \bar{\psi}\tau_j\psi - 2i\bar{\psi}(\vec{\theta} \times \vec{\tau})_j\psi$
 $\Rightarrow (\bar{\psi}\vec{\tau}\psi)^2 \rightarrow (\bar{\psi}\vec{\tau}\psi)^2 + \mathcal{O}(\theta^2)$

- similar manipulations for the kaonic field \mathcal{K} lead to the same result:

$$(\mathcal{K}^\dagger \vec{\tau} \mathcal{K})^2 \rightarrow (\mathcal{K}^\dagger \vec{\tau} \mathcal{K})^2 + \mathcal{O}(\theta^2)$$

- and evidently: $(\vec{\rho}_\mu)^2 \rightarrow (\vec{\rho}_\mu)^2 + \mathcal{O}(\theta^2)$

Since our Lagrangian density (2.1) contains only terms with $\vec{\rho}^2$ -like behavior, the rotations in the isospin space are symmetry transformations.

The conserved current associated with this transformation reads:

$$\begin{aligned} \vec{j}_\mu = & \lambda_N \bar{\psi} \gamma_\mu \vec{\tau} \psi + \lambda_R \vec{\rho}^\nu \times \vec{R}_{\mu\nu} \\ & + \lambda_K \mathcal{K}^\dagger \vec{\tau} \left\{ i \overleftrightarrow{\partial}_\mu + 2g_{\omega K} [g_{\omega K} \omega_\mu + g_{\rho K} \vec{\tau} \cdot \vec{\rho}_\mu + g_{\phi K} \phi_\mu + e \frac{1}{2}(1 + \tau_3) A_\mu] \right\} \mathcal{K}, \end{aligned} \quad (\text{B.11})$$

for any arbitrary $\lambda_N, \lambda_R, \lambda_K \in \mathbb{R}$.

Using these results and equations of motion for massive vector meson fields, which follow from the Lagrangian density (2.1):

$$\partial_\mu F_{\mu\nu} - m_\Phi \Phi_\nu = j_\nu^{(\Phi)}, \quad (\text{B.12})$$

where $j_\nu^{(\Phi)}$ is a conserved current, we can show that:

$$\partial^\nu \partial^\mu F_{\mu\nu} - m_\Phi \partial^\nu \Phi_\nu = \partial^\nu j_\nu^{(\Phi)}, \quad (\text{B.13})$$

and thus:

$$\partial_\nu \Phi^\nu = 0 \quad (\text{B.14})$$

for any $\Phi_\mu \in \{\omega_\mu, \vec{\rho}_\mu, \phi_\mu\}$.

For massless photon field, one has a freedom of gauge transformation:

$$A_\mu \rightarrow A_\mu + \partial_\mu f, \quad (\text{B.15})$$

which can be constrained by Lorentz condition:

$$\partial_\mu A^\mu = 0. \quad (\text{B.16})$$

C Numerical solution

⁵ Although the baryon field in (2.11) is still an operator, the meson fields are classical. It means that Dirac equation is linear and we can seek normal-mode solutions of the form:

$$\psi(x) = e^{-i\varepsilon t} \psi(\vec{x}).$$

This leads to:

$$\begin{aligned} \mathcal{H} \psi(\vec{x}) &= \varepsilon \psi(\vec{x}) \\ \mathcal{H} &= [-i\alpha_j \nabla_j + (m_N - g_{\sigma N} \sigma) \beta + g_{\omega N} \omega_0 + g_{\rho N} \tau_3 \rho_0 + e \frac{1}{2} (1 + \tau_3) A_0], \end{aligned} \quad (\text{C.1})$$

where \mathcal{H} is the single-particle Dirac Hamiltonian. Considering both positive and negative energy solutions $u_\alpha(\vec{x})$ and $v_\alpha(\vec{x})$, the baryon field operator can be expanded as:

$$\hat{\psi}(\vec{x}) = \sum_{\alpha} \hat{a}_{\alpha} u_{\alpha}(\vec{x}) + \hat{b}_{\alpha}^{\dagger} v_{\alpha}(\vec{x}) \quad (\text{C.2})$$

in the Schrödinger picture. Here, $\hat{a}_{\alpha}^{\dagger}$ and $\hat{b}_{\alpha}^{\dagger}$ are creation operators for baryons and antibaryons, respectively. The label α specifies the full set of quantum numbers describing the single-particle solutions. Since the system is assumed spherically symmetric and parity conserving, α contains the angular momentum and parity quantum numbers (for details see e.g. Ref. [48]).

For the the single-particle angular momentum operator:

$$\vec{J} = \vec{L} + \vec{S} = \vec{x} \times \vec{p} + \frac{1}{2} \vec{\Sigma}, \quad (\text{C.3})$$

where $\Sigma^i = (i/2)\varepsilon_{ijk}\gamma^j\gamma^k$ or:

$$\vec{\Sigma} = \begin{pmatrix} \vec{\sigma} & 0 \\ 0 & \vec{\sigma} \end{pmatrix}, \quad (\text{C.4})$$

it holds:

$$[\mathcal{H}, J_i] = [\mathcal{H}, \vec{J}^2] = 0, \quad \text{for } i = 1, 2, 3, \quad (\text{C.5})$$

⁵Following text was partly adopted from Ref. [37] and modified in order to incorporate antikaons.

i.e., \mathcal{H} is rotationally invariant. Consequently, the j and m quantum numbers of the angular momentum may be used to label the states. Although \vec{L}^2 does not commute with \mathcal{H} , the spin operator $\vec{S}^2 = \vec{\Sigma}^2/4$ obeys $[\mathcal{H}, \vec{S}^2] = 0$, so the spin $s = 1/2$ is another constant of motion. Moreover, if we define the operator:

$$\mathcal{K} = \gamma^0[\vec{\Sigma} \cdot \vec{J} - 1/2] = \gamma^0[\vec{\Sigma} \cdot \vec{L} + 1] \quad (\text{C.6})$$

then $[\mathcal{H}, \mathcal{K}] = 0$, which also provides a constant of motion. Since:

$$\mathcal{K}^2 = \vec{L}^2 + \vec{\Sigma} \cdot \vec{L} + 1 = \vec{J}^2 + 1/4 \quad (\text{C.7})$$

it follows that the eigenvalues ($-\kappa$) of the operator \mathcal{K} obey:

$$\kappa = \pm(j + 1/2) \quad (\text{C.8})$$

and κ is a nonzero integer. If we act on the upper and lower two-component wave function

$$\psi = \begin{pmatrix} \psi_A \\ \psi_B \end{pmatrix} \quad (\text{C.9})$$

with the operator \mathcal{K} :

$$\mathcal{K}\psi = -\kappa\psi = \begin{pmatrix} -\kappa\psi_A \\ -\kappa\psi_B \end{pmatrix} = \begin{pmatrix} (\vec{\sigma} \cdot \vec{L} + 1)\psi_A \\ -(\vec{\sigma} \cdot \vec{L} + 1)\psi_B \end{pmatrix}, \quad (\text{C.10})$$

i.e., ψ_A and ψ_B are eigenstates of $(\vec{\sigma} \cdot \vec{L} + 1)$ with opposite eigenvalues. For $\vec{L}^2 = \vec{J}^2 - \vec{\Sigma} \cdot \vec{L} - 3/4$, it follows that:

$$\begin{aligned} \vec{L}^2\psi_A &= [(j + 1/2)^2 + \kappa]\psi_A \equiv l_A(l_A + 1)\psi_A, \\ \vec{L}^2\psi_B &= [(j + 1/2)^2 - \kappa]\psi_B \equiv l_B(l_B + 1)\psi_B. \end{aligned} \quad (\text{C.11})$$

Thus, although ψ is not an eigenstate of \vec{L}^2 , the upper and lower components are separately eigenstates. For given j and κ , the values of l may be determined from:

$$\begin{aligned} j(j + 1) - l_A(l_A + 1) + 1/4 &= -\kappa, \\ j(j + 1) - l_B(l_B + 1) + 1/4 &= \kappa. \end{aligned} \quad (\text{C.12})$$

Since the two-component wave functions have fixed j and $s = 1/2$, l_A and l_B must be $j \pm 1/2$. Their angular momentum and spin parts are therefore spherical harmonics:

$$\begin{aligned} \Phi_{\kappa m} &= \sum_{m_l m_s} \langle l m_l 1/2 m_s | l 1/2 j m \rangle Y_{l m_l}(\theta, \phi) \chi_{m_s} \\ j = |\kappa| - 1/2, \quad l &= \begin{cases} \kappa & \kappa > 0 \\ -(\kappa + 1) & \kappa < 0 \end{cases}, \end{aligned} \quad (\text{C.13})$$

where $Y_{l m_l}$ is a spherical harmonics and χ_{m_s} is a two-component Pauli spinor. For a given κ , eq. (C.8) and the first relation in (C.12) uniquely determine j and l , as indicated in (C.13). Thus the single-particle wave functions in a central, parity-conserving field may be written as:

$$\psi_\alpha(\vec{x}) = \psi_{n\kappa m t}(\vec{x}) = \begin{pmatrix} i [G_{n\kappa t}(r)/r] \Phi_{\kappa m} \\ -[F_{n\kappa t}(r)/r] \Phi_{-\kappa m} \end{pmatrix} \zeta_t. \quad (\text{C.14})$$

Since the Hamiltonian \mathcal{H} also commutes with the isospin operator T_3 and \vec{T}^2 , the states may be labeled by their charge or isospin projection t ($t = 1/2$ for protons, $t = -1/2$ for neutrons), and ζ_t is a two-component isospinor. The principal quantum number is denoted by n . The phase choice in (C.14) leads to real bound state wave functions F and G for real potentials in eq. (C.1).

Using the general form of the solutions (C.14), we evaluate the local source terms in the meson field equations. We assume that the ground state consists of filled shells up to some n and κ . (This is consistent with spherical symmetry and is appropriate for doubly magic nuclei.) In addition, we assume that all bilinear products of baryon operators are normal ordered.

With these assumptions, the baryon density becomes:

$$\begin{aligned} \rho_v(r) &= \langle : \hat{\psi}^\dagger(\vec{x}) \hat{\psi}(\vec{x}) : \rangle \\ &= \sum_{\alpha}^{occ} u_\alpha^\dagger(\vec{x}) u_\alpha(\vec{x}) \\ &= \sum_a^{occ} \left(\frac{2j_a + 1}{4\pi r^2} \right) [|G_a(r)|^2 + |F_a(r)|^2], \end{aligned} \quad (\text{C.15})$$

where $a \equiv \{n, \kappa, t\}$ denotes remaining quantum numbers. The other densities may be calculated analogously.

With these results, we rewrite the meson field equations as:

$$\begin{aligned}
\left(\frac{d^2}{dr^2} + \frac{2}{r} \frac{d}{dr} - m_\sigma^2\right) \sigma(r) &= -g_{\sigma N} \rho_s(r) \\
&\quad - g_2 \sigma^2(r) + g_3 \sigma^3(r) - g_{\sigma K} m_K \rho_{K^-}^{(s)}(r) \\
&= -g_{\sigma N} \sum_a^{\text{occ}} \left(\frac{2j_a + 1}{4\pi r^2}\right) [|G_a(r)|^2 - |F_a(r)|^2] \\
&\quad - g_2 \sigma^2(r) + g_3 \sigma^3(r) - g_{\sigma K} m_K \rho_{K^-}^{(s)}, \\
\left(\frac{d^2}{dr^2} + \frac{2}{r} \frac{d}{dr} - m_\omega^2\right) \omega(r) &= -g_{\omega N} \rho_v(r) + d\omega^3(r) + g_{\omega K} \rho_{K^-}(r), \\
&= -g_{\omega N} \sum_a^{\text{occ}} \left(\frac{2j_a + 1}{4\pi r^2}\right) [|G_a(r)|^2 + |F_a(r)|^2], \\
&\quad + d\omega^3(r) + g_{\omega K} \rho_{K^-}(r) \\
\left(\frac{d^2}{dr^2} + \frac{2}{r} \frac{d}{dr} - m_\rho^2\right) \rho(r) &= -g_{\rho N} \rho_3(r) + g_{\rho K} \rho_{K^-}(r), \\
&= -g_{\rho N} \sum_a^{\text{occ}} \left(\frac{2j_a + 1}{4\pi r^2}\right) [|G_a(r)|^2 + |F_a(r)|^2] (-1)^{t_a - 1/2}, \\
&\quad + g_{\rho K} \rho_{K^-}(r) \\
\left(\frac{d^2}{dr^2} + \frac{2}{r} \frac{d}{dr} - m_\omega^2\right) \phi(r) &= +g_{\phi K} \rho_{K^-}(r), \\
\left(\frac{d^2}{dr^2} + \frac{2}{r} \frac{d}{dr}\right) A(r) &= -e \rho_p(r) + e \rho_{K^-}(r) \\
&= -e \sum_a^{\text{occ}} \left(\frac{2j_a + 1}{4\pi r^2}\right) [|G_a(r)|^2 + |F_a(r)|^2] (t_a + 1/2) \\
&\quad + e \rho_{K^-}(r),
\end{aligned} \tag{C.16}$$

where the densities are given in (2.13).

The equations for baryon wave functions follow immediately upon substituting (C.14) into (C.1):

$$\begin{aligned}
\frac{d}{dr} G_a(r) + \frac{\kappa}{r} G_a(r) - [E_a - g_{\omega K} \omega(r) - t_a g_{\rho N} \rho(r) \\
-(t_a + \frac{1}{2}) e A(r) + M - g_{\sigma N} \sigma(r)] F_a(r) = 0,
\end{aligned} \tag{C.17}$$

$$\begin{aligned} \frac{d}{dr} F_a(r) - \frac{\kappa}{r} G_a(r) + [E_a - g_{\omega K} \omega(r) - t_a g_{\rho N} \rho(r) \\ - (t_a + \frac{1}{2}) e A(r) - M + g_{\sigma N} \sigma_0(r)] G_a(r) = 0. \end{aligned} \quad (\text{C.18})$$

The normalization condition for nucleons reads:

$$\int dr (|G_a(r)|^2 + |F_a(r)|^2) = 1. \quad (\text{C.19})$$

The coupled nonlinear differential equations (2.11) have to be solved by an iterative procedure. For a given trial set of meson fields, the Dirac equations (C.18) are solved by Runge-Kutta integration, integrating outward from the origin and inward from large r , matching solutions at some intermediate radius to determine the eigenvalue E_a . Analytic solutions in the regions of large and small r allow proper boundary conditions to be imposed. The Klein-Gordon equation for the antikaon is solved with this trial set of meson fields as well, with the reasonable estimate of the antikaon energy E_{K^-} .

Once the baryon and antikaon wave functions are determined, the source terms in the meson Klein-Gordon equations are calculated and the meson fields recomputed by integrating over the static Green's function:

$$D(r, r'; m_i) = -\frac{1}{m_i r r'} \sinh(m_i r_{<}) \exp(-m_i r_{>}). \quad (\text{C.20})$$

The Green's function embodies the boundary conditions of exponential decay at large r and vanishing slope for the fields at origin. For example, the solution of the Klein-Gordon equation for the scalar field reads:

$$\begin{aligned} \sigma(r) = \int dr' r'^2 [-g_{\sigma N} \rho_s(r') - g_2 \sigma^2(r') + g_3 \sigma^3(r') - g_{\sigma K} m_K K^*(r') K(r')] \times \\ \times D(r, r'; m_\sigma). \end{aligned} \quad (\text{C.21})$$

The new meson fields are then introduced in the equations of motion for nucleons and the antikaon. The entire procedure is repeated until selfconsistency is achieved.